T7 DNA polymerase treatment improves quantitative sequencing of both double-stranded and single-stranded DNA viruses

Maud Billaud[1], Ilias Theodorou[1,3], Quentin Lamy-Besnier[1], Shiraz A. Shah[4], François Lecointe[1], Luisa De Sordi[2,3], Marianne De Paepe[1] and Marie-Agnès Petit[1*]

1. Université Paris-Saclay, INRAE, Micalis unit, Jouy en Josas France
2. Sorbonne Université, INSERM, Centre de Recherche St Antoine, Paris, France
3. Paris Center for Microbiome Medicine (PaCeMM) FHU, AP-HP, Paris, France.
4. Copenhagen Prospective Studies on Asthma in Childhood, Copenhagen University Hospital, Herlev-Gentofte, Ledreborg Allé 34, DK-2820 Gentofte, Denmark

*Corresponding author, marie-agnes.petit@inrae.fr

Summary

Background: Bulk microbiome, as well as virome-enriched shotgun sequencing only reveals the double-stranded DNA (dsDNA) content of a given sample, unless specific treatments are applied. However, genomes of viruses often consist of a circular single-stranded DNA (ssDNA) molecule. Pre-treatment and amplification of DNA using the multiple displacement amplification (MDA) method enables conversion of ssDNA to dsDNA, but this process can lead to over-representation of these circular ssDNA genomes. A more recent alternative permits to bypass the amplification step, as library adapters are ligated to sheared and denatured DNA, after an end-modification step (xGen kit). However, the sonication step might shear ssDNA more efficiently than dsDNA, therefore introducing another bias in virome sequencing. These limitations prompted us to explore an alternative method of DNA preparation for sequencing mixed ssDNA and dsDNA viromes.

Methods: We present here a new method for sequencing both ssDNA and dsDNA, using the T7 DNA polymerase (T7pol) to convert ssDNA into dsDNA. We compared this method to two others: short MDA, where the amplification step is limited by a 30-minute instead of 90-minute incubation time, and no pre-treatment before the xGen kit for library preparation. These various methods were first applied on synthetic a mixtures, then the most effective one was applied on virome samples.

Results: Our findings indicate that the T7pol method better represents the original synthetic mixtures compared to the other methods. Furthermore, when applied to two complex virome samples, the T7pol treatment improved both the richness and abundance in the *Microviridae* fraction.

Conclusion: We conclude that T7pol pretreatment is preferable to MDA for the shotgun sequencing of viromes, which is easy to implement and inexpensive.

Keywords:

T7 DNA polymerase, shotgun sequencing, single-stranded DNA

51 ***Background***

52 In the last ten years, many methodological improvements have helped generate informative
53 metagenomics datasets for the virus-enriched fraction (or virome) of any type of environmental or
54 biological sample (Castro-Mejia et al., 2015; Deng et al., 2019; Hsieh et al., 2021; Shkoporov et al.,
55 2018; Wang et al., 2022). A particular difficulty of virome sequencing lies in the fact that the genetic
56 material of viruses is not exclusively made of double-stranded (ds) DNA, as is the case for bacteria
57 and higher organisms. It is frequently composed of single-stranded (ss) DNA and ss- or dsRNA. To our
58 knowledge, a single method allowing the preparation of all these substrates at once for deep
59 sequencing is not yet available. Even the simpler challenge of disposing of a method for the
60 sequencing of both ds and ssDNA viruses is not completely solved.

61 Initially, most viromes were sequenced after a multiple displacement amplification (MDA) step,
62 which was a convenient way to increase the usually low amounts of viral DNA to quantities
63 compatible with library preparation. It became rapidly obvious that MDA introduced a bias favoring
64 small and circular ssDNA viral genomes (the smallest ssDNA genomes are approximately 2000 nt
65 long, while larger inoviruses are approximately 7000 nt long) (Kim and Bae, 2011; Yilmaz et al., 2010).
66 This is because the Phi29 DNA polymerase used for MDA has potent strand displacement activity
67 (Blanco et al., 1989). Therefore, once these small ssDNA genomes are converted into dsDNA, the
68 polymerase proceeds for further rounds, generating long concatemers. Tests with synthetic mixes of
69 viral genomes unambiguously demonstrated this caveat of MDA for mixes of ss- and dsDNA genomes
70 (Roux et al., 2016).

71 Two main solutions were proposed to circumvent this problem. First, the "short MDA (sMDA)"
72 method consisted of reducing the incubation time of the MDA treatment from the normally
73 recommended 90-120 minutes to 30 minutes (Deng et al., 2019). The second solution consisted of
74 replacing the amplification step with a library kit able to add adapters to ssDNA molecules. Here,
75 after an initial shearing step, all DNA molecule extremities, both ss- and dsDNA, receive a short
76 extension using an "adaptase", the nature of which is kept secret by the manufacturer. Then, an
77 additional linker is added, allowing PCR amplification and sample labeling. This methodology is used
78 in the Accel-NGS kit from Swift Biosciences (recently acquired by Integrated DNA Technologies (IDT)
79 and rebranded as the xGen kit, below xGen). It was initially developed for the sequencing of ancient
80 DNA, and has started to be used in the virome community (Roux et al., 2016). For this second
81 method, tests with synthetic mixes showed that the bias in favor of ssDNA viruses was significantly
82 reduced (Roux et al., 2016).

83 Using the xGen kit also comes with a drawback: the DNA shearing step is performed before the
84 conversion of ssDNA to dsDNA, which may result in discrepancies if ssDNA is more readily sheared
85 than dsDNA. This leads to possible downstream biases in library preparations, which require a
86 homogeneous size distribution of the DNA fragments.

87 This prompted us to search for an alternative method of DNA preparation for the sequencing of
88 mixed ssDNA and dsDNA viromes. We present here this new method based on the use of T7 DNA
89 polymerase (T7pol) and compare it to two other methods: sMDA amplification, or no pretreatment.
90 Then, all libraries were prepared with the xGen kit, for comparison purposes. We first compared the
91 performance of the three methods on a synthetic community of five phages, and then tested the
92 new T7Pol pre-treatment method followed by xGen libraries on two human viromes, in comparison
93 with samples that had not been pre-treated.

94

95

96 ***Methods***

97 *DNA, enzymes, oligonucleotides, kits and other materials*

98 ssDNA of M13mp18 and PhiX174, as well as dsDNA of PhiX174, were purchased from New England
99 Biolabs (NEB, references N4040S, N3023L and N3021S, respectively). T7pol was purchased from NEB
100 (ref. M0274) and used following the manufacturer's instructions. Turbo DNAse I was purchased from
101 Thermo Fisher Scientific (reference AM2222), and benzonase from Millipore (purity > 90%, reference
102 70746). For MDA treatments, the Genomiphi2 kit was purchased from Fisher Scientific (reference
103 10628505). The "xGen ssDNA Low-Input DNA Lib Prep 16rxn" (previously, Accel NGS S2 kit) was
104 purchased from IDT (reference 10009859). Random oligonucleotides of a 20-nt size were purchased
105 from Eurofins Genomics. SPRI Select magnetic beads were purchased from Beckman Coulter
106 (reference B23318). To filter out bacteria from lysates and samples, polyethersulfone (PES) syringe
107 filters 0.8/0.2 µm were used (Pall corporation, reference 4187).

108 *Phage lysates preparations*

109 Two *Escherichia coli* infecting phages with ssDNA genomes were selected for the study: PhiX174 and
110 an M13 derivative. PhiX174 is a *Microviridae* that forms a tail-less icosaedric capsid enclosing its
111 circular 5386 nt ssDNA genome. It was grown on *E. coli* strain C, which codes for its appropriate core
112 LPS receptor (Feige and Stirm, 1976). M13-yfp (De Paepe et al., 2010) is a filamentous phage of the
113 *Inoviridae* family harboring a 7916 nt long circular ssDNA genome. It was grown on *E. coli* strain
114 MG1655 F'kanR, a strain coding for the F pilus, which is the M13 receptor. Three dsDNA
115 Caudoviricetes were also selected for the study: SPP1, T4 and lambda. T4 and lambda are *Escherichia*
116 *coli*-infecting phages and were grown on *E. coli* strain MG1655. Inside the virions, the T4 genome is a
117 169 kb-long, linear dsDNA molecule, while the lambda linear genome has a shorter, 48 kb-long linear
118 dsDNA genome. Finally, the *Bacillus subtilis* infecting phage SPP1 was propagated on strain YP886,
119 generating virions containing a linear, 46 kb-long genome.

120 Phage lysates of T4, SPP1, lambda and phiX174 were prepared as described previously (Sausset et al.,
121 2022), and bacterial remains were removed by centrifugation (5000 g, 7 min, 4°C), followed by
122 filtration through PES filters. A lysate of M13-yfp was obtained by propagating the infected strain in
123 50 mL of LB-broth Lennox (Formedium) with 50 µg/mL kanamycin up to OD_{600} 1, removing bacteria
124 by centrifugation (5000 g, 7 min, 4°C), and filtering the supernatant with PES filter. Stocks were kept
125 at 4°C in salt-magnesium (SM) buffer (200 mM NaCl, 50 mM Tris pH 7.5, 10 mM $MgSO_4$).

126 *Pure phage DNA preparation*

127 From lysates, phages were concentrated by overnight centrifugation (20 000 g, 16 h), resuspended in
128 0.5 mL SM buffer, and loaded on SM-iodixanol gradients as described (Sausset et al., 2022). The
129 phage-containing fraction was dialyzed against SM buffer and stored at 4°C. Prior to phage DNA
130 extraction, purified particles were treated for 1 h at 37°C with DNaseI (8 units) and RNaseA (20 units)
131 in SM buffer complemented with 0.5 mM $CaCl_2$ to eliminate any residual bacterial DNA or RNA. The
132 reaction was stopped by adding EDTA (20 mM).

133 To extract DNA from the capsids, samples were then treated with proteinase K (2 mg/mL) and SDS
134 (0.5%) for 20 min at 56°C. Phage DNA was then extracted by phenol-chloroform-isoamyl alcohol
135 (25:24:1) extraction followed by two chloroform-isoamyl alcohol (24:1) purification steps. At each
136 step, the solvent and aqueous phases were separated by centrifugation 15 minutes at 12 000g, 4°C.
137 DNA was then supplemented with 300 mM potassium acetate pH 4.8, and precipitated with two
138 volumes of ethanol, centrifuged for 30 min at 12000 g and 4°C, and the pellet was resuspended in
139 10 mM Tris buffer pH 8. Phage dsDNA concentration was estimated using a Qubit device.

140 *Phage quantification and preparation of the synthetic phage mixes*

141 To prepare mixes containing phages in known concentrations, phage genome quantities of T4,
142 lambda, SPP1 and PhiX174 were determined by qPCR, in comparison to dilutions of pure DNA
143 standards. For these standards, concentration of PhiX174 ssDNA (from NEB) was verified with a
144 spectrophotometer (Nanodrop). For dsDNA qPCR standards, highly purified phage stocks of T4, SPP1
145 and lambda were prepared and quantified as described in the "Pure phage DNA preparation"
146 section. Next, each stock of pure DNA was diluted in 10 mM Tris pH 8 to obtain a concentration of
147 $5x10^6$ phage genomes in 6 µL. The samples were further diluted four times by 3-fold dilution steps, to
148 obtain the calibration range ($1.8x10^5$ to $5x10^6$ genomes), and aliquots stored at -20°C until use.
149 Prior to quantify the four phage lysates, they were treated with DNaseI using 1 µL of enzyme/ml
150 phage sample (1 h at 37°C) to eliminate any residual free DNA, and then treated at 95°C for 5
151 minutes, for capsid denaturation. Primers indicated in supplementary table 1 were used at a
152 concentration of 200 nM. Three dilutions of each heat-denatured phage stock were compared to the
153 calibration curves of highly purified DNA of the corresponding phage, as described above. qPCR was
154 performed in a total volume of 15 µL (6 µL purified DNA or phage particle dilution and 9 µL of
155 amplification mix) in MicroAmp Fast Optical 96-well plates sealed with MicroAmp Optical Adhesive
156 Film (both from Applied Biosystems, reference 4346906 and 4311971, respectively) using the Luna
157 universal qPCR master mix (NEB, ref M3003). Amplifications were run in duplicate on a StepOnePlus
158 real-time PCR system with the following cycling conditions: 95°C for 5 min, (95°C for 15 s, 58°C for 45
159 s, 72°C for 30 s) for 45 cycles, 72°C for 5 min, 95°C for 15 s, 60°C for 15 s, and 95°C for 15 s. The
160 analysis of the melting curves confirmed the specificity of the primers. Data analysis was performed
161 with StepOne software 2.3.
162
163 The M13-yfp lysate could not be quantified by qPCR due to coat resistance to heat (González-Cansino
164 et al., 2019), so it was quantified by plaque formation units on the MG1655 F'kan strain. Plaque
165 counts of M13-yfp were easy to determine, as it is an M13mp18 derivative making much clearer
166 plaques than the parental M13. Once each phage stock had been quantified, synthetic mixes were
167 prepared. Initial phage concentrations in each stock, as well as volumes added to compose each mix,
168 are presented in supplementary table 2.
169
170 *Synthetic mixes DNA extractions*

171 To extract the DNA from the two synthetic mixes, an initial volume of 500 µL was used and DNA was
172 extracted by phenol-chloroform treatment, as described in the "pure phage DNA preparation"
173 section., resuspended in 25 µL of 10 mM Tris (pH 8), and dispatched twice for the three treatments
174 as follows: 1 µL for MDA pretreatment (according to the Genomiphi2 kit instructions), 5 µL for T7pol
175 pretreatment, and 5 µL for the xGen library without pretreatment. Final DNA yields were in average
176 100 ng for untreated and T7pol treated samples, 25 ng for the Genomiphi amplified mix with low
177 proportion of ssDNA, and 500 ng for the Genomiphi amplified mix with high proportion of ssDNA.

178
179 *T7pol pretreatment*
180
181 Primers for T7pol priming should have a minimum length of 15 nt (Hernandez et al., 2016), and their
182 optimal size is 21 nt (C.C. Richardson, personal communication). To test whether degenerated
183 primers could be used with T7pol to convert any phage ssDNA to dsDNA, degenerated primers of 20
184 nt were tested on ssDNA from PhiX174 and M13mp18. For the annealing step, samples containing
185 250 ng of M13mp18 and 250 ng of PhiX174 ssDNA in a final volume of 25 µL of water were incubated
186 with varying concentrations of oligonucleotides for 5 minutes at 65°C (primer concentrations are
187 indicated at this first annealing step, samples are then diluted 2-fold for the replication step). The
188 samples were then allowed to cool down slowly by disposing them on floaters over a beaker
189 containing 25 mL of 65°C water and placed at room temperature until final temperature was below

190 46°C (usually 10 minutes). Replication was then initiated by adding 300 µM dNTPs, 1X T7pol buffer,
191 50 µg/mL BSA and 5 units of T7pol in each tube completed with water to a final volume of 50 µL,
192 followed by incubation for 5 minutes at 37°C. Reactions were stopped by placing the samples at 75°C
193 for 20 minutes. Prior gel loading, samples were adjusted to 0.2% SDS, 10 mM EDTA and 0.5 mg/mL
194 proteinase K, and incubated at 50°C for 30 minutes, to remove proteins that might prevent proper
195 migration of the DNA molecules. Products (15 µL) were separated on a 0.7% agarose gel containing
196 40 µg/mL ethidium bromide. For the T7pol pretreatment of phage DNA mixes, the same conditions
197 were applied, except that degenerated primers were used at a final concentration of 10 µM,
198 together with 5 µL of DNA mix complemented with water to a final volume of 25 µL. The next
199 replication step was performed in a final volume of 50 µL with 5 units of T7pol.
200
201 *Effect of sonication and magnetic bead size selection on ss- and dsDNA*
202
203 PhiX174 ssDNA and dsDNA were each diluted at 20 ng/µL into 100 µL volumes and treated for
204 sonication using conditions applied for library preparation (see below). Half of each sample was then
205 submitted to SPRIselect magnetic bead binding, using conditions removing dsDNA fragments below
206 200 bp, as applied for library preparation (see below), except that elution was done in the same 50
207 µL volume of Tris 10 mM pH 8. To visualize ssDNA fragment sizes, products were then separated on a
208 10 cm-long polyacrylamide denaturing gel (5% of acryl/bis 19:1, 8 M urea, 1 x TBE). For this, 10 µL of
209 formamide stained with bromophenol blue was added to 10 µL of each sample, incubated at 90°C for
210 5 minutes, and then placed on ice. Samples (20 µL) were then loaded on a preheated gel (>1 hour
211 migration, 450 volts) and separated for ~20 minutes at 300 volts until bromophenol blue reached the
212 gel border. The gel was stained for 30 minutes with Syber Gold (Invitrogen, reference S11494, 1X
213 final concentration), and bands were revealed by a Bio-Rad ChemiDocTM MP imaging system. The
214 size at the maximum signal intensity of each smear was estimated with Image Lab software (Bio-Rad
215 Laboratories). Six PCR fragments 601, 440, 330, 279, 200 and 116 bp-long were denatured with
216 formamide and run as a size ladder.
217
218 *Library preparations, synthetic phage mix sequencing and analysis*
219
220 DNA preparations from the synthetic phage mixes were first pretreated (or not) for the conversion of
221 ssDNA to dsDNA using either the Phi29 polymerase of the Genomiphi2 kit according to the supplier's
222 instructions with a 30-minute incubation or T7pol (see Results section). Next, all samples were
223 sonicated (100 µL in 1.5 mL tubes) with a Diagenode Bioruptor Pico device in a cooled water bath
224 (4°C) for 21 sec with 90 sec breaks for 3 cycles, centrifuged to collect droplets on the side of the
225 tubes, and sonicated again for 21 sec with 90 sec breaks for 2 cycles to generate DNA segments of an
226 average size of approximately 500 bp. DNA samples were then concentrated to 20 µL using
227 SPRIselect magnetic beads from Beckman Coulter (ratio beads/DNA=1.2) to remove fragments below
228 200 bp. All samples were then processed for library preparation using the xGen kit, following the
229 manufacturer's instructions. These library steps included (1) adaptase (37°C, 15 min then 95°C, 2
230 min); (2) extension (98°C, 30 s; 63°C, 15 s; 68°C, 5 min); (3) magnetic bead cleaning; (4) linker ligation
231 (25°C, 15 min); (5) magnetic bead cleaning; (6) DNA concentration estimation by Qubit (high
232 sensitivity kit); and (7) indexing by PCR (98°C, 30 s followed by 4 to 14 cycles of 98°C, 10 s; 60°C, 30 s;
233 68°C, 60 s) depending on the initial DNA concentration.
234
235 Paired-end sequencing (2x150 nt) was performed on an Illumina ISeq100 system at a depth of
236 800 000 reads per sample. Read cleaning was then computed with fastp (v 0.23.1, (Chen et al., 2018))
237 using the following parameters: --trimfront2 15 --trimtail1 2 --trimtail2 2 –trim_poly_g –trim_poly_x
238 –r –W 4 –M 20 –u 30 –e 20 –l 100 –p –w 12. These parameters were used to remove the adapters
239 present at read extremities with xGen libraries. Read mapping of both paired and unpaired reads on
240 the phage genomes was then conducted with bwa (Li and Durbin, 2009) and the –a parameter. Next,
241 the data were treated and analyzed with msamtools and the following parameters: msamtools filter
242 –b –u –l 80 –p 95 –z 80 –besthit –S and then msamtools profile –multi=proportional. The number of

243 reads mapped per genome was normalized in relative abundance (rel) at the msamtools profile step
244 using the default parameter. Rel are computed as follows: an “abundance” value of each genome is
245 estimated by the number of reads mapped to that genome, divided by its length and normalized by
246 the sum of abundances across all five genomes. The proportion of each phage within the sequenced
247 sample was then estimated by this rel ratio.
248
249 To compare final compositions of the sequenced mixes, Aitchison distances were used. This distance
250 is a Euclidean distance based on centered log ratio (CLR) transformations of a virus count matrix. CLR
251 transformation accounts for the compositionality that is especially pronounced when only a few taxa
252 are present. In such cases Aitchison distances provide the most accurate metric for gauging the
253 similarity of samples.
254
255 *Human fecal virome sample preparation and treatment*

256 Fecal samples (0.2 g) from two healthy donors S4 and S18 were first resuspended in 4 mL of 10 mM
257 Tris, pH 7.5, and then centrifuged (5 200 g, 30 min, 4°C). The supernatant was filtered using 0.2 µm
258 diameter PES filters. Then, a benzonase-nuclease treatment (75 U per sample) was performed for 2 h
259 at 37°C. The viral samples were then concentrated by precipitation overnight at 4°C using
260 polyethyleneglycol (PEG 8000, 10% w/v) and NaCl 0.5 M. After centrifugation (5 200 g, 1 h, 4°C), the
261 pellet was retrieved and processed for DNA extraction as described in the “Pure phage DNA
262 preparation” section. Each DNA sample was then divided into two parts: one was kept unprocessed,
263 and the other was further treated with T7pol as described above. All samples libraries were then
264 prepared with the xGen kit. Paired-end sequencing (2x150 nt) was performed on an Illumina
265 platform at a depth of 5 million read pairs per sample.

266 *Bioinformatics analysis of the virome samples*

267 The different steps of the analysis are summarized in supplementary figure 1. First, reads were
268 cleaned with fastp as described for the synthetic mix sequencing, above. To remove contamination,
269 all the reads mapping to the human genome (GRCh38) according to Bowtie2 (v 2.4.1, (Langmead and
270 Salzberg, 2012)) with the --very-sensitive option were then excluded. The remaining reads were
271 assembled using SPAdes (options --only assembler -k 21,33,55,77,99,127, v 3.15.3, (Prjibelski et al.,
272 2020)). Deduplication of contigs at the species level (95% average nucleotide identity) was performed
273 using BLAT (Kent, 2002) as previously published (Shah et al., 2023). Viral contigs were identified
274 through two parallel approaches: using softwares and searching by alignment against Refseq, as well
275 as recently released phage gut databases. For the software, VirSorter2 (options --include-groups
276 dsDNAphage,NCLDV,RNA,ssDNA,lavidaviridae --exclude-lt2gene --min-length 2000 --viral-gene-
277 required --hallmark-required --min-score 0.9 --high-confidence-only, v 2.2.3, (Guo et al., 2021),
278 VIBRANT (default parameters, v 1.2.1, (Kieft et al., 2020)), and CheckV (v 0.8.1, database v 1.5,
279 (Nayfach et al., 2021a)) were used. For CheckV, only the contigs with a minimum of "medium" quality
280 were considered viral. Contigs classified as viral by any of these three softwares (with the mentioned
281 parameters) were kept. For the databases, contigs were aligned using BLAT (v 36, (Kent, 2002))
282 against the following databases: COPSAC (Shah et al., 2023), GVD (Gregory et al., 2020), MGV
283 (Nayfach et al., 2021b), GPD (Camarillo-Guerrero et al., 2021) and viral RefSeq. The contigs that
284 aligned against any contig in the databases with an alignment length >= 80% of the database contig
285 were considered viral. A list of unique viral OTUs was generated by combining the outputs of both of
286 these approaches. Gene calling on viral contigs was performed with Prodigal (Hyatt et al., 2010).
287 *Microviridae* were identified among all these viral contigs by searching for the presence of either the
288 major capsid protein (MCP) or replication initiation protein (Rep). For this, we ran HHsearch (Soding,
289 2005) against specific PHROGs profiles (PHROG 514 for the MCP, and PHROGs 713 and 942 for Rep),
290 and retained hits with at least 90% probability and 60% coverage of the target protein (Terzian et al.,

291 2021). To retrieve a closer relative for the identified *Microviridae*, a vContact2 graph was constructed
292 (Bin Jang et al., 2019), which included these contigs and INPHARED (March 2023 version) as
293 reference database (Cook et al., 2021). This graph was then analyzed with graphanalyzer (Pandolfo et
294 al., 2022). For comparison purposes, the four samples were then subsampled to 2 M paired-end
295 reads per sample using seqtk (v 1.3, https://github.com/lh3/seqtk). The subsampled reads were then
296 aligned against the set of viral contigs using BWA-mem2 (v 2.2.1, (Vasimuddin et al., 2019)) with the -
297 a option. Then, using msamtools, reads were first filtered to only keep alignments > 80 bp with >95%
298 identity over >80% read length and only keeping the best alignment for each read (options -l 80 -p 95
299 -z 80 –besthit). To exclusively work with contigs for which there is sufficient support of its presence in
300 a given sample, only contigs for which the overall sequencing depth was >= 1 and at least 50% of the
301 contig length was covered were kept (values computed using msamtools coverage –summary
302 command). The relative abundance of each contig passing these criteria was determined by using the
303 msamtools profile (options --multi=proportional --unit=rel). At the end of these treatments, sample
304 S4 contained 269 viral OTUs when no T7pol treatment had been applied, and 181 viral OTU for the
305 T7pol pretreatment sample. Sample S18 was richer, with 645 and 702 vOTU without and with T7pol
306 treatment, respectively. Those relative abundances were finally analyzed using the R package
307 phyloseq (v 1.38.0, (McMurdie and Holmes, 2013)).

308

309 ***Results***

310 *Comparing the fate of ssDNA and dsDNA during library preparations*

311 A necessary step of library preparations involves the production of DNA fragments of a
312 homogeneous size, either by enzymatic treatment or ultrasonic DNA shearing. Enzymatic treatment
313 cannot target ssDNA, and ssDNA treatment by sonication may result in systematic lower sizes
314 compared to dsDNA. Indeed, the xGen protocol mentions that fragmentation of ssDNA may result in
315 shorter fragments and lower library yields. To quantify this difference, samples of dsDNA and ssDNA
316 corresponding to the RF1 replicating form and the virion form of the phage PhiX174 genome,
317 respectively, were sonicated in parallel (replicates performed on two different days) for the duration
318 applied during library preparation and separated on a urea-denaturing 5% acrylamide gel. After
319 sonication, a lower size of DNA strands was systematically observed for the ssDNA samples
320 compared to the dsDNA samples (peak size at 316 versus 562 nt for replicate 1 and 235 versus 330 nt
321 for replicate 2, Figure 1: ds and ss slots).

322 Some protocols concentrate the sonicated aliquots to 20 µL using magnetic beads for the adaptase
323 step of the xGen kit (see Methods). We tested whether ssDNA fragments were preferentially lost at
324 this step as well. Using the PhiX174 sonicated samples, total DNA recovery after the bead cleaning
325 step was estimated with a Nanodrop apparatus. Whereas a total loss of 42-48% relative to input DNA
326 was found for the dsDNA samples, this loss was more pronounced for ssDNA samples (74-84%).
327 Migration of these samples next to their untreated controls on the denaturing gel indicated that this
328 preferential loss was due to a higher size cutoff for ssDNA, compared to dsDNA, as the size at peak
329 intensity increased after bead treatment for ssDNA (from 316 to 407 nt in replicate 1 and from 235 to
330 325 nt in replicate 2, Figure 1: ss and ssB labels), unlike for dsDNA (Figure 1: ds and dsB labels).

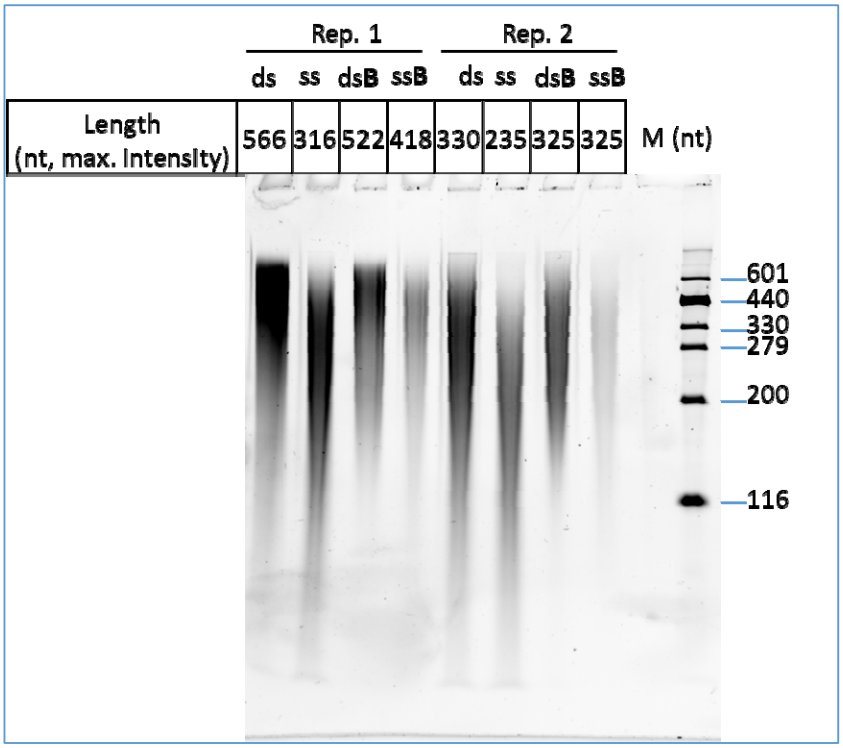

Figure 1. Effect of sonication and SPRI magnetic beads on ssDNA (ss slots) and dsDNA (ds slots) of PhiX174. All samples were sonicated for 5 cycles of 21 seconds, and a half volume was then treated with SPRI magnetic beads (B slots) to remove fragments below 200 bp. Samples were separated on a 5% acrylamide urea-denaturing gel. M: size marker. See the original gel picture in supplementary figure 2.

331 We concluded that both sonication and magnetic bead treatments had differential effects on ss- and
332 dsDNA, with ssDNA being cut to 56-71% of the average size of dsDNA and small fragment removal by
333 magnetic beads leading to a 2-fold lower recovery of ssDNA fragments compared to dsDNA.

334 *Setting up a ssDNA-to-dsDNA conversion protocol using T7 DNA polymerase.*

335 To limit any bias in the treatments of ss- versus dsDNA molecules, we therefore searched for a
336 quantitative method to convert ssDNA molecules to dsDNA prior to sonication. Contrary to the Phi29
337 DNA polymerase, T7pol has no intrinsic strand displacement activity, and does not open up the DNA
338 strands ahead of polymerization process (Blanco et al., 1989; Canceill et al., 1999; Lechner and
339 Richardson, 1983) (Figure 2A). Instead, a separate, replicative DNA helicase is responsible for this
340 step, as in most living organisms (Canceill et al., 1999). As a consequence, once a first round of

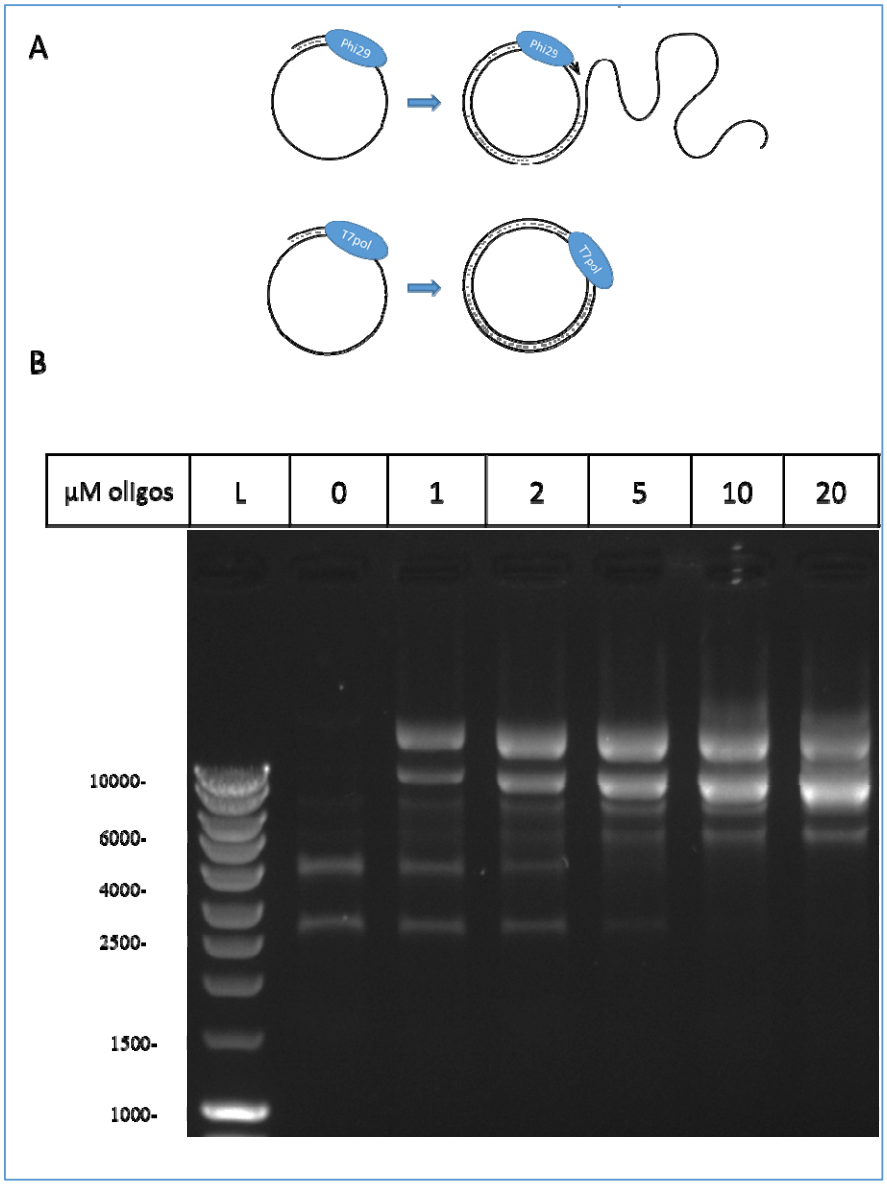

Figure 2: A. The different strand displacement activities of Phi29 DNA polymerase (up, rolling circle) and T7pol (down, stops after one round). B. Adjusting primer concentrations for T7pol conversion of ssDNA to dsDNA of M13 and PhiX174. Degenerated oligonucleotides (20 nt) were annealed at the indicated concentrations on a mix of M13 and PhiX174 ssDNA and incubated in the presence of T7pol. Products separated on 0.7% agarose gel are shown. Sizes (bp) of linear dsDNA standards (lane L, Smart ladder, Eurogentec) are indicated on the left (bp). See the original gel picture in supplementary figure 3.

341 replication has been completed on a circular ssDNA molecule, T7pol stops and unloads, therefore
342 preventing DNA overamplification.

343 To test conditions allowing T7pol replication initiation using degenerated oligonucleotides as
344 primers, a 1:1 weight mix of PhiX174 and M13mp18 circular ssDNA molecules was used (10 µg/mL
345 final DNA concentration). A range of oligonucleotide concentrations from 1 to 20 µM was tested. We
346 found that 10 µM of 20 nt long degenerated oligonucleotides were sufficient to convert all the ssDNA
347 species into dsDNA (Figure 2B). In addition, and as expected, no smear indicative of further rounds of
348 replication beyond the first one was detected. The marked intensity of the dsDNA bands, relative to
349 ssDNA, was due to the higher affinity of ethidium bromide for dsDNA.

350 We concluded that T7pol treatment of circular and ssDNA should be an efficient and quantitative
351 way to convert all DNA molecules to dsDNA prior to library preparation.

352 *A T7pol pretreatment of synthetic viromes generates more accurate results*

353 We therefore proceeded to test this T7pol treatment on mock phage mixes and compared it to other
354 ways of treating DNA for library preparation. For this, two synthetic mixes were prepared from stocks
355 of five phages, two of which were ssDNA phages (M13-yfp and PhiX174), and three dsDNA phages
356 (T4, lambda and SPP1). One mix contained 48.4% of ssDNA phage genomes (45.3% of M13-yfp, 3.1%
357 of PhiX174), while the other contained only 5.9% of ssDNA phage genomes (5.5% M13-yfp and 0.4%

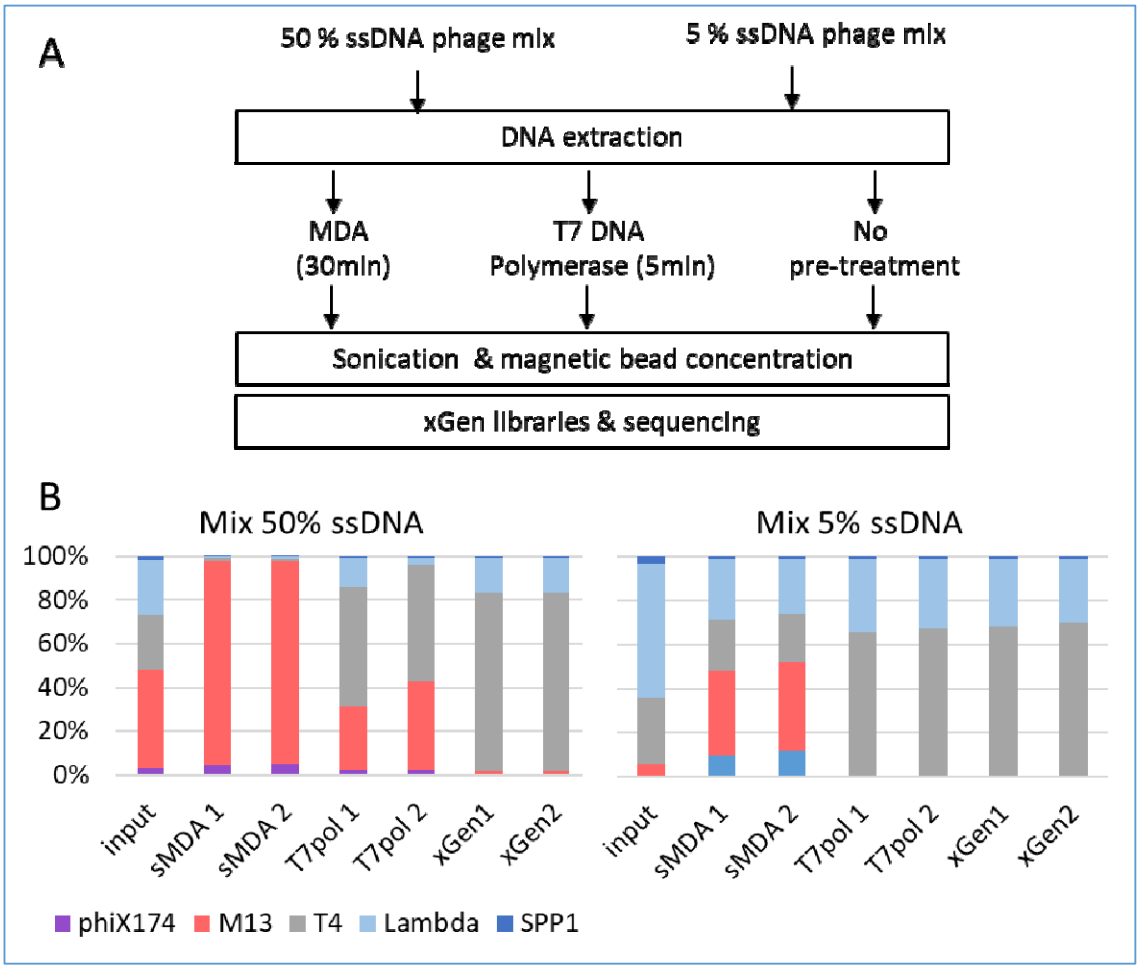

Figure 3. A: Comparison of protocols for sequencing ss- and dsDNA mixes. B. Input bar: Theoretical initial proportions of the 5 phages. Next six bars: Observed proportions of the 5 phages after deep sequencing (in duplicate, 1 and 2) of xGen DNA libraries either pre-treated with sMDA, T7pol, or without pre-treatment (xGen). Relative abundances are shown (rel values, see Methods).

358 PhiX174). The final and global phage concentration in each mix was approximately 10^9 genomes/mL
359 to mimic realistic viral concentrations in fecal samples (assuming a 10-fold dilution of fecal matter at
360 10^{10} particles/g).

361 Next, DNA was extracted from the two mixes, and each was subjected to one of the three following
362 treatments (Figure 3A): (i) short MDA (sMDA), (ii) T7pol-dependent DNA replication using an excess
363 of 10 µM degenerated oligonucleotides, and (iii) no pretreatment. Then, all samples were sonicated
364 in a final volume of 100 µL and concentrated using magnetic beads. Finally, all were processed with
365 the xGen kit for library preparation (see Methods for details). Each treatment was performed in
366 duplicate, and the 12 samples were then sequenced on an Illumina platform. Read mapping on the 5
367 phage genomes was converted into relative abundances, to estimate the proportion of each phage in
368 the mix at the end of all treatments and to compare them to their theoretical initial ratio (Figure 3B,
369 and supplementary table 3).

370 We found that the DNA samples treated directly with xGen libraries (absence of pretreatment) led to
371 a major depletion of the ssDNA phages: starting with the 48.4% input ssDNA mix, ssDNA phages only
372 contributed 1.8-1.9% of the final sequencing result. The reduction of the ssDNA mix was even more
373 drastic with 5.9% input ssDNA, as no reads matching the two ssDNA phages were obtained in one of
374 the replicates, and M13 contributed only 0.09% of the sequenced virome in the other experiment.
375 Since input DNA strands for library preparation were twice less abundant for ssDNA phages relative
376 to dsDNA phages, the overall ssDNA phage depletion was 10-fold for the high input mix and over 30-
377 fold for the low input mix.

378 With the short MDA pretreatment, starting with the 48.4% input ssDNA mix, 98% of ssDNA phage
379 genomes were recovered, and 48-52% were recovered when using the 5.9% input ssDNA mix (here
380 and below, no correction for single-strand molecules was applied, as all molecules were in the dsDNA
381 state for library preparation). We conclude that overamplification occurred in both cases by factors
382 of 2 and 8.6, respectively.

383 Finally, the T7pol pretreatment gave a result that was more congruent with input DNA: for the 48.4%
384 ssDNA input mix, similar proportions (31-43%) of ssDNA phage were recovered, and 8.2-fold lower
385 ssDNA (0.7%) was found for the 5.9% input mix.

386 To quantify the congruence between the initial mix compositions and the different pretreatments
387 while accounting for the compositionality of the data, we computed Aitchison distances, a metric
388 used to compare ecosystem compositions (Aitchison, 1982). Distances obtained between each input
389 DNA mix and the various outputs, using the abundances from supplementary table 3, are reported in
390 Table 1.

391 Table 1: A. Aitchison distances between the compositions obtained from the different pretreatments and the
392 input composition with low ssDNA amounts (5.9%). B. Same calculations for the high ssDNA input mix.

A.	Mix low ssDNA
xGen 1	8.17
xGen 2	5.97
sMDA 1	3.86
sMDA2	4.02
T7pol 1	2.29
T7pol 2	2.23

B.	Mix high ssDNA
xGen 1	3.72
xGen 2	3.93
sMDA 1	4.39
sMDA 2	4.34
T7pol 1	2.15
T7pol 2	2.31

393

394 T7pol pretreatment was more quantitative than both other methods, regardless of the input
395 ssDNA/dsDNA ratio. Among the two other methods, short MDA pretreatment was more quantitative
396 than direct xGen libraries for the mix with a low ssDNA concentration. However, the opposite was
397 true at higher ssDNA concentrations. As a reference, the distance between the two input mixes
398 themselves was also computed and found to be 3.05. This indicates that the T7pol pretreatment gave
399 results closer to its initial mix (a distance of approximately 2) than the distance between the two
400 input stocks.

401 *T7pol treatment of two viromes*

402 To investigate the effect of T7pol treatment on complex environmental samples, two fecal samples
403 were collected from healthy individuals (S4 and S18). Viromes were prepared, DNA extracted, and
404 each sample was then treated or not with T7polprior to sequencing, following the protocol described
405 above. xGen libraries were then prepared exactly as for the synthetic communities. Reads were
406 assembled de novo in contigs, which were then processed for the identification of viral ones. Among
407 them, *Microviridae* were recognized by the presence of either the major capsid protein-encoding
408 gene or the replication gene (see supplementary table 4 and supplementary figure 5 for details on
409 these contigs). Mapping back the reads on all viral contigs allowed to determine the relative
410 abundance of *Microviridae*. For the first sample, the relative abundance of *Microviridae* increased
411 from 24% to 74% of all viral contigs upon T7pol treatment. Richness in *Microviridae* also slightly
412 increased, from 28 to 33 species. We noted, however, that 6 of the *Microviridae* contigs detected in
413 the untreated samples were not present in the T7pol sample, while conversely, 11 *Microviridae*
414 contigs were found only in the T7pol sample. A detailed analysis of the *Microviridae* profile indicated
415 that each microvirus contig gained some level of abundance (some 8 +/- 6-fold on average), as
416 indicated in Figure 4A (see also supplementary table 5). For the second sample, the relative
417 abundance of microviral species among viral contigs increased from 25% to 30%, and richness shifted
418 from 5 to 8 species (Fig. 4B and supplementary table 5). We therefore conclude that the T7pol
419 treatment improves overall the detection of *Microviridae* in complex samples, marginally in one case,
420 and more substantially in the other case. Conversely, relative abundances of dsDNA, Caudoviricetes
421 contigs were reduced upon T7pol treatment in sample S4. Their abundance was mostly unchanged in
422 sample S18 (supplementary figure 4 and supplementary table 6). This was expected, as these two
423 categories represent most of the signal, and therefore mirror each other in human fecal samples.
424 T7pol treatment therefore allows for better detection of ssDNA phages in natural samples, in
425 agreement with the results obtained for synthetic communities.

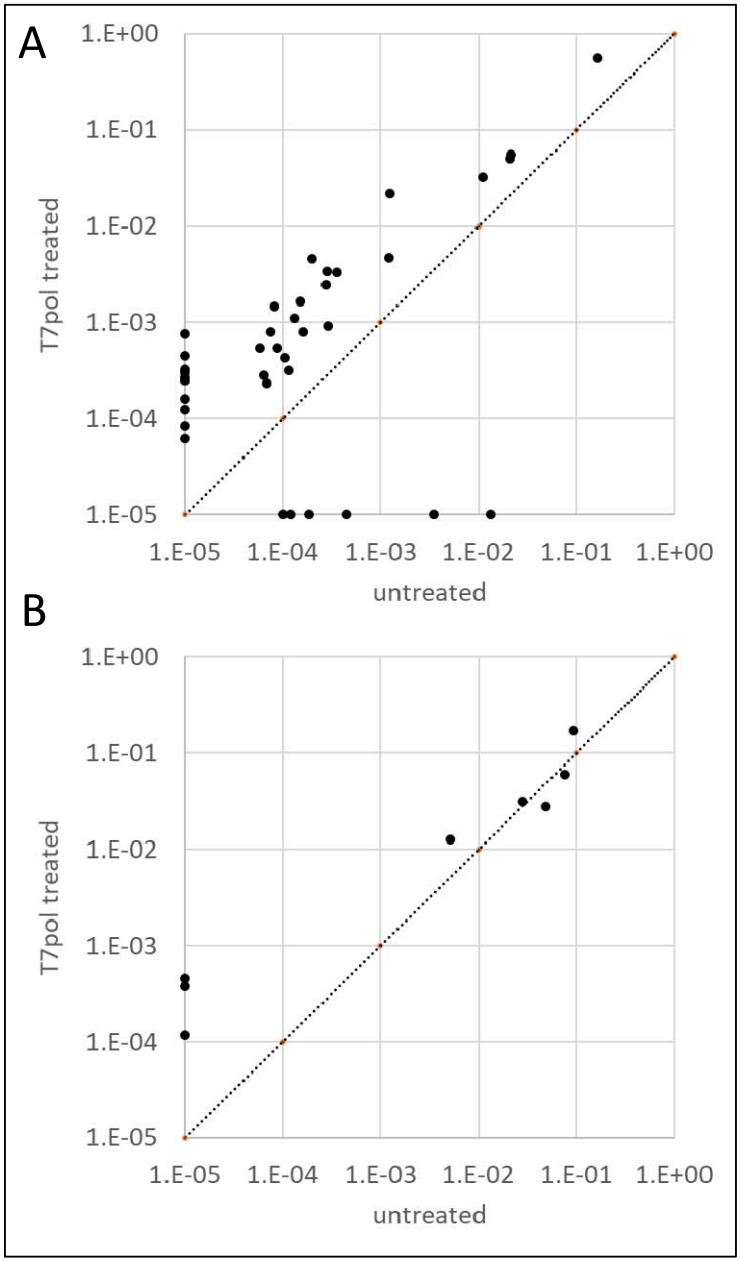

Figure 4: Relative abundance of each *Microviridae* detected in samples S4 (panel A) and S18 (panel B). Each dot represents one contig, with its abundance relative to all phages of the sample when sequenced without prior treatment for ssDNA (X axis) or after T7pol treatment (Y axis). The dotted line shows the bisector. Contigs undetected with one of the treatments were assigned an artificial value of 10^{-5}.

426

427 ***Discussion***

428 In the present benchmarking experiment, xGen libraries performed on untreated sonicated DNA
429 were the most detrimental to ssDNA sequencing: ssDNA was recovered at levels 10 to over 30-fold
430 less than expected. A previous study that also used synthetic mixes to compare MDA and xGen
431 methods concluded that ssDNA sequencing was quantitative with xGen libraries (Roux et al., 2016).
432 Many subtle differences might have led to the different conclusions. First, in a previous report, phage
433 concentrations were estimated by epifluorescence, a method that might have underestimated the
434 two *Microviridae* phage concentrations (PhiX174 and Alp3), as these particles are particularly dim
435 under the microscope. Second, the kit used for DNA extraction (QIAamp DNA Mini Kit) was said to
436 recover only 27% of the DNA for dsDNA phages while providing full recovery of ssDNA phages, so
437 that proportions of dsDNA phages were artificially inflated *a posteriori*. In the present work, a
438 phenol–chloroform extraction protocol was used, and no *a posteriori* corrections were made. Third,
439 we found that ssDNA was more sensitive to shearing during the sonication step, and the parameters
440 are likely to vary between sonication procedures. Fourth, we showed that some ssDNA was lost in
441 our protocol at the magnetic bead step after sonication (the details of library preparation are not
442 mentioned in (Roux et al., 2016)). Clearly, all steps of DNA treatments should be carefully tested to
443 ensure proper recovery of ssDNA. Nevertheless, our observation confirms the notion that
444 pretreatments permitting the conversion of all ssDNA molecules to dsDNA prior to sonication should
445 limit downstream bias, such as those we observed here. Having all DNA in the dsDNA state at the
446 onset of library preparation also permits more accurate DNA concentration measurements, which is
447 key for the tuning of sonication parameters, according to each kit supplier's instructions.

448 MDA was the first method used to convert ssDNA to dsDNA; however, this method has long been
449 known to be detrimental for the quantitative assessment of viromes containing a mix of ss- and
450 dsDNA genomes (Kim and Bae, 2011; Roux et al., 2016). The standard 90-120 minute incubation time
451 used for MDA was reported to amplify ssDNA by an excess of 33 to 44-fold when the input ssDNA
452 was 2% (Roux et al., 2016). We found, however, that a shortening of the incubation time to 30
453 minutes (designated here "sMDA") somewhat reduces the bias favoring ssDNA genomes: they were
454 only in 8.6-fold excess when starting from 5.9% input ssDNA. However, starting with 48.4% ssDNAled
455 to final ssDNA proportion of 98% of all sequenced DNA, somehow hiding all remaining dsDNA phage
456 content.

457 T7pol pretreatment appears to be a better method than sMDA for sequencing DNA viromes. The
458 overall distance between the final sequencing product and the input DNA was the least in this case,
459 as well as being the most consistent between both tested compositions. In particular, with respect to
460 ssDNA, the final ssDNA genome proportions were only slightly lower than input ssDNA when the
461 input phage mix had a high proportion of ssDNA (48.4%). However, for the low input ssDNA mix, the
462 final proportion was 8.2-fold lower than expected. It may be that the annealing step required for
463 T7pol-mediated DNA replication is less efficient when the ssDNA molecules are a minority within a
464 complex sample. We also observed an improvement in the detection of *Microviridae*, which have
465 ssDNA genomes, in two human fecal viromes sequenced with xGen libraries when applying the T7pol
466 pretreatment. This shows that such a treatment is feasible on natural samples and reinforces the
467 interest in such a method.

468 It should be noted, however, that none of the protocols tested allowed the generation of an accurate
469 image of the relative proportions of the five input phages of the two synthetic communities. This
470 should be kept in mind when applying ecological metrics such as diversity and richness to viral
471 metagenomics data. Compared to bacterial metagenomics, ecological analysis based on viral
472 metagenomics is still in its infancy.

473 The T7pol pretreatment adds only a marginal cost (~1 euro per sample) to the library preparations
474 compared to a Genomiphi MDA pretreatment (20 euros per sample). Moreover, it should be possible
475 to apply it to samples planned for any kind of downstream library preparation kit for low DNA
476 amounts, such as the Nextera or TruSeq DNA nano kits from Illumina, making it independent of the
477 25% more expensive xGen kit, which was used here for comparison purposes. Further analyses are
478 needed to explore this possibility.

479 Furthermore, the T7pol method described here might be a useful addition in the future for projects
480 aiming at simultaneously describing the bacterial and viral components of their microbial ecosystems
481 without missing ssDNA viruses. In fact, several large databases of phage contigs have already been
482 generated thanks to the data mining of shotgun metagenomics (Camarillo-Guerrero et al., 2021;
483 Gregory et al., 2020; Nayfach et al., 2021b; Tisza et al., 2021). Such studies rely on the sorting of viral
484 contigs among all other microbial contigs based on their characteristics and gene contents (Guo et
485 al., 2021; Kieft et al., 2020). While this method is certainly efficient in detecting prophages, as well as
486 phage DNA replicating inside bacteria and possibly encapsidated DNA, ssDNA phage genomes will
487 probably escape analysis, as no pretreatment step ensuring their conversion into dsDNA is
488 performed at present (Camarillo-Guerrero et al., 2021; Nayfach et al., 2021b; Tisza et al., 2021). We
489 noted, however, that *Microviridae* were sometimes present in studies assembling viral sequences
490 from shotgun metagenomic samples which, in theory, should not have sequenced ssDNA (Camarillo-
491 Guerrero et al., 2021; Nayfach et al., 2021b; Tisza et al., 2021). This might be explained if dsDNA
492 replication intermediates were extracted together with bacterial DNA. We cannot exclude, however,
493 that, depending on the biochemistry of each library preparation kit, the ssDNA fraction might be
494 included unknowingly, and sequenced quantitatively. The present work shows that in any case,
495 adding a T7 polymerase pretreatment can improve the sequencing of ssDNA viruses.

496

497 ***Conclusion:*** We conclude that T7pol pretreatment is a better alternative to MDA for the shotgun
498 sequencing of both the dsDNA and ssDNA fractions of viromes, which is easy to implement and
499 inexpensive.

500 ***Declarations***

501 *Ethics approval and consent to participate.* Approval for human studies was obtained from the local
502 ethics committee (Comité de Protection des Personnes Ile-de-France IV, IRB 00003835 Suivitheque
503 study; registration number 2012/05NICB).

504 *Consent for publication.* Not applicable

505 *Availability of data and material*: The supplementary material (all supplementary figures and tables),
506 as well as the raw reads generated for this study are available at https://doi.org/10.57745/C0BAPR.

507 *Competing interests:* The authors declare they have no competing interests.

508 *Funding:* This work was funded by INRAE and Sorbonne Université, as well as the ANR project
509 PRIMAVERA.

510 *Authors' contributions:* MB, IT, QLB and FL conceived and realized the experiments, analyzed the data
511 and contributed to the redaction of the manuscript. MAP supervised the research and wrote the
512 manuscript. MDP and LDS supervised the research and contributed to the redaction of the
513 manuscript. SAS contributed to the statistical analysis of the data and to the redaction of the
514 manuscript.

515 Acknowledgments: The Migale platform at INRAE, on which bioinformatics analyses were conducted,
516 is warmly thanked for its constant support and help.

References

Aitchison, J. (1982). The Statistical Analysis of Compositional Data. Journal of the Royal Statistical Society Series B (Methodological) *44*, 139-177.

Bin Jang, H., Bolduc, B., Zablocki, O., Kuhn, J.H., Roux, S., Adriaenssens, E.M., Brister, J.R., Kropinski, A.M., Krupovic, M., Lavigne, R.*, et al.* (2019). Taxonomic assignment of uncultivated prokaryotic virus genomes is enabled by gene-sharing networks. Nat Biotechnol *37*, 632-639.

Blanco, L., Bernad, A., Lazaro, J.M., Martin, G., Garmendia, C., and Salas, M. (1989). Highly efficient DNA synthesis by the phage phi 29 DNA polymerase. Symmetrical mode of DNA replication. J Biol Chem *264*, 8935-8940.

Camarillo-Guerrero, L.F., Almeida, A., Rangel-Pineros, G., Finn, R.D., and Lawley, T.D. (2021). Massive expansion of human gut bacteriophage diversity. Cell *184*, 1098-1109 e1099.

Canceill, D., Viguera, E., and Ehrlich, S.D. (1999). Replication slippage of different DNA polymerases is inversely related to their strand displacement efficiency. J Biol Chem *274*, 27481-27490.

Castro-Mejia, J.L., Muhammed, M.K., Kot, W., Neve, H., Franz, C.M., Hansen, L.H., Vogensen, F.K., and Nielsen, D.S. (2015). Optimizing protocols for extraction of bacteriophages prior to metagenomic analyses of phage communities in the human gut. Microbiome *3*, 64.

Chen, S., Zhou, Y., Chen, Y., and Gu, J. (2018). fastp: an ultra-fast all-in-one FASTQ preprocessor. Bioinformatics *34*, i884-i890.

Cook, R., Brown, N., Redgwell, T., Rihtman, B., Barnes, M., Clokie, M., Stekel, D.J., Hobman, J., Jones, M.A., and Millard, A. (2021). INfrastructure for a PHAge REference Database: Identification of Large-Scale Biases in the Current Collection of Cultured Phage Genomes. Phage (New Rochelle) *2*, 214-223.

De Paepe, M., De Monte, S., Robert, L., Lindner, A.B., and Taddei, F. (2010). Emergence of variability in isogenic Escherichia coli populations infected by a filamentous virus. PLoS One *5*, e11823.

Deng, L., Silins, R., Castro-Mejia, J.L., Kot, W., Jessen, L., Thorsen, J., Shah, S., Stokholm, J., Bisgaard, H., Moineau, S.*, et al.* (2019). A Protocol for Extraction of Infective Viromes Suitable for Metagenomics Sequencing from Low Volume Fecal Samples. Viruses *11*.

Feige, U., and Stirm, S. (1976). On the structure of the *Escherichia coli* C cell wall lipopolysaccharide core and on its phiX174 receptor region. Biochem Biophys Res Commun *71*, 566-573.

González-Cansino, J.L., Vieyra-Eusebio, M.T., Vera-Robles, L.I., and Hernández-Arana, A. (2019). Environmental adjustments of the cooperativity in M13 phage thermal denaturation. Thermochimica Acta *672*, 53-59.

Gregory, A.C., Zablocki, O., Zayed, A.A., Howell, A., Bolduc, B., and Sullivan, M.B. (2020). The Gut Virome Database Reveals Age-Dependent Patterns of Virome Diversity in the Human Gut. Cell Host Microbe *28*, 724-740 e728.

Guo, J., Bolduc, B., Zayed, A.A., Varsani, A., Dominguez-Huerta, G., Delmont, T.O., Pratama, A.A., Gazitua, M.C., Vik, D., Sullivan, M.B.*, et al.* (2021). VirSorter2: a multi-classifier, expert-guided approach to detect diverse DNA and RNA viruses. Microbiome *9*, 37.

Hernandez, A.J., Lee, S.J., and Richardson, C.C. (2016). Primer release is the rate-limiting event in lagging-strand synthesis mediated by the T7 replisome. Proc Natl Acad Sci U S A *113*, 5916-5921.

Hsieh, S.Y., Tariq, M.A., Telatin, A., Ansorge, R., Adriaenssens, E.M., Savva, G.M., Booth, C., Wileman, T., Hoyles, L., and Carding, S.R. (2021). Comparison of PCR versus PCR-Free DNA Library Preparation for Characterising the Human Faecal Virome. Viruses *13*.

Hyatt, D., Chen, G.L., Locascio, P.F., Land, M.L., Larimer, F.W., and Hauser, L.J. (2010). Prodigal: prokaryotic gene recognition and translation initiation site identification. BMC Bioinformatics *11*, 119.

Kent, W.J. (2002). BLAT--the BLAST-like alignment tool. Genome Res *12*, 656-664.

Kieft, K., Zhou, Z., and Anantharaman, K. (2020). VIBRANT: automated recovery, annotation and curation of microbial viruses, and evaluation of viral community function from genomic sequences. Microbiome *8*, 90.

Kim, K.H., and Bae, J.W. (2011). Amplification methods bias metagenomic libraries of uncultured single-stranded and double-stranded DNA viruses. Appl Environ Microbiol *77*, 7663-7668.

Langmead, B., and Salzberg, S.L. (2012). Fast gapped-read alignment with Bowtie 2. Nat Methods *9*, 357-359.

Lechner, R.L., and Richardson, C.C. (1983). A preformed, topologically stable replication fork. Characterization of leading strand DNA synthesis catalyzed by T7 DNA polymerase and T7 gene 4 protein. J Biol Chem *258*, 11185-11196.

Li, H., and Durbin, R. (2009). Fast and accurate short read alignment with Burrows-Wheeler transform. Bioinformatics *25*, 1754-1760.

McMurdie, P.J., and Holmes, S. (2013). phyloseq: an R package for reproducible interactive analysis and graphics of microbiome census data. PLoS One *8*, e61217.

Nayfach, S., Camargo, A.P., Schulz, F., Eloe-Fadrosh, E., Roux, S., and Kyrpides, N.C. (2021a). CheckV assesses the quality and completeness of metagenome-assembled viral genomes. Nat Biotechnol *39*, 578-585.

Nayfach, S., Paez-Espino, D., Call, L., Low, S.J., Sberro, H., Ivanova, N.N., Proal, A.D., Fischbach, M.A., Bhatt, A.S., Hugenholtz, P.*, et al.* (2021b). Metagenomic compendium of 189,680 DNA viruses from the human gut microbiome. Nat Microbiol *6*, 960-970.

Pandolfo, M., Telatin, A., Lazzari, G., Adriaenssens, E.M., and Vitulo, N. (2022). MetaPhage: an Automated Pipeline for Analyzing, Annotating, and Classifying Bacteriophages in Metagenomics Sequencing Data. mSystems *7*, e0074122.

Prjibelski, A., Antipov, D., Meleshko, D., Lapidus, A., and Korobeynikov, A. (2020). Using SPAdes De Novo Assembler. Curr Protoc Bioinformatics *70*, e102.

Roux, S., Solonenko, N.E., Dang, V.T., Poulos, B.T., Schwenck, S.M., Goldsmith, D.B., Coleman, M.L., Breitbart, M., and Sullivan, M.B. (2016). Towards quantitative viromics for both double-stranded and single-stranded DNA viruses. PeerJ *4*, e2777.

Sausset, R., Krupova, Z., Guédon, E., Peron, S., Grangier, A., Petit, M.-A., De Sordi, L., and De Paepe, M. (2022). Comparison of interferometric light microscopy with nanoparticle tracking analysis for the study of extracellular vesicles and bacteriophages. Journal of Extracellular Vesicles.

Shah, S.A., Deng, L., Thorsen, J., Pedersen, A.G., Dion, M.B., Castro-Mejia, J.L., Silins, R., Romme, F.O., Sausset, R., Jessen, L.E.*, et al.* (2023). Expanding known viral diversity in the healthy infant gut. Nat Microbiol.

Shkoporov, A.N., Ryan, F.J., Draper, L.A., Forde, A., Stockdale, S.R., Daly, K.M., McDonnell, S.A., Nolan, J.A., Sutton, T.D.S., Dalmasso, M.*, et al.* (2018). Reproducible protocols for metagenomic analysis of human faecal phageomes. Microbiome *6*, 68.

Soding, J. (2005). Protein homology detection by HMM-HMM comparison. Bioinformatics *21*, 951-960.

Terzian, P., Olo Ndela, E., Galiez, C., Lossouarn, J., Perez Bucio, R.E., Mom, R., Toussaint, A., Petit, M.A., and Enault, F. (2021). PHROG: families of prokaryotic virus proteins clustered using remote homology. NAR Genom Bioinform *3*, lqab067.

Tisza, M.J., Belford, A.K., Dominguez-Huerta, G., Bolduc, B., and Buck, C.B. (2021). Cenote-Taker 2 democratizes virus discovery and sequence annotation. Virus Evol *7*, veaa100.

Vasimuddin, M., Misra, S., Li, H., and Aluru, S. (2019). Efficient architecture-awar acceleration of BWA-MEM for multi-core systems. Paper presented at: IEEE International parallel and distributed processing symposium (IPDPS) (Rio de Janeiro, Brazil).

Wang, G., Li, S., Yan, Q., Guo, R., Zhang, Y., Chen, F., Tian, X., Lv, Q., Jin, H., Ma, X.*, et al.* (2022). Optimization and evaluation of viral metagenomic amplification and sequencing procedures toward a genome-level resolution of the human fecal DNA virome. J Adv Res.

Yilmaz, S., Allgaier, M., and Hugenholtz, P. (2010). Multiple displacement amplification compromises quantitative analysis of metagenomes. Nat Methods *7*, 943-944.

517 Supplementary table 1: Primers used for qPCR

Phage	Forward	Reverse	Reference
T4	ACTGGCCAGGTATTCGCA	ATGCTTCTTTAGCACCGGCA	[12]
lambda	GAGTGCGGAAGATGCAAAGG	TTAACAGTGCGTGACCAGG	[13]
SPP1	CGGGCTGAAATACCTGTGGA	TAGCCCCTCCTCCGATTGTT	[14]
PhiX174	GGTTCGTCAAGGACTGGTT	TTGAACAGCATCGGACTCAG	this work

518
519
520
521
522 Supplementary table 2: Synthetic mix preparations

Phage	initial stock	volume added for each mix (µL)		ratio of each phage	
	phage/mL	Mix high ssDNA	Mix low ssDNA	Mix high ssDNA	Mix low ssDNA
T4	3.3E+09	370.2	370.2	24.9%	30.1%
lambda	7.5E+10	16.5	32.9	25.2%	60.8%
SPP1	5.4E+09	13.2	23.7	1.5%	3.2%
phiX174	4.7E+09	32.1	32.1 (dil 10x)	3.1%	0.4%
M13-yfp	3.0E+10	73.8	73.8 (dil 10x)	45.3%	5.5%

523

524 Supplementary table 3: Proportion of the five genomes in input mixes and after sequencing, using
525 the different protocols. A panel, high ssDNA mix, B panel, low ssDNA mix.

A. high ssDNA mix	input	short MDA 1	short MDA 2	T7pol 1	T7pol 2	xGen without pretreatment 1	xGen without pretreatment 2
T4 (ds)	24.9%	1.2%	1.0%	54.8%	53.6%	81.4%	81.4%
Lambda (ds)	25.2%	0.8%	0.9%	13.4%	2.9%	16.2%	16.2%
SPP1 (ds)	1.5%	0.0%	0.0%	0.5%	0.7%	0.6%	0.6%
PhiX174 (ss)	3.1%	4.7%	5.1%	2.6%	2.5%	0.2%	0.1%
M13-yfp (ss)	45.3%	93.3%	92.9%	28.6%	40.2%	1.7%	1.7%
%ssDNA, in total	48.4%	98.0%	98.0%	31.3%	42.7%	1.9%	1.8%

526

B. low ssDNA mix	input	short MDA 1	short MDA 2	T7pol 1	T7pol 2	xGen without pretreatment 1	xGen without pretreatment 2
T4 (ds)	30.1%	23.3%	22.2%	65.3%	66.5%	68.1%	69.7%
Lambda (ds)	60.8%	27.5%	24.9%	33.1%	31.9%	31.0%	29.5%
SPP1 (ds)	3.2%	1.0%	1.0%	1.0%	1.0%	0.9%	0.7%
PhiX174 (ss)	0.4%	9.8%	11.4%	0.2%	0.1%	0.00%	0.00%
M13-yfp (ss)	5.5%	38.4%	40.3%	0.5%	0.6%	0.00%	0.09%
%ssDNA, in total	5.9%	48.2%	51.7%	0.7%	0.7%	0.0%	0.1%

527

528

Contig	CheckV Quality	Length	GC%	Closer Relative	HostGenus
Microvirus_01	High-quality	5816	47.54	Human gut gokushovirus	NA
Microvirus_02	Medium-quality	4309	38.8	NA	Prevotella
Microvirus_03	Medium-quality	4289	38.7	NA	Prevotella
Microvirus_04	Complete	5961	43.9	Microviridae sp.	Faecalibacterium
Microvirus_05	Complete	5454	44.98	Sigmofec virus UA08Rod_5824	NA
Microvirus_06	Complete	7094	36.31	Microvirus sp.	Prevotella
Microvirus_07	Complete	5880	43.59	Poophage MBI-2016a	NA
Microvirus_08	Medium-quality	3185	36.17	NA	NA
Microvirus_09	High-quality	6650	40.33	Dipodfec virus UOA04_Rod_446	NA
Microvirus_10	High-quality	5925	44.1	Dipodfec virus UOA04_Rod_841	NA
Microvirus_11	Complete	6229	40.78	Microviridae sp.	Phocaeicola
Microvirus_12	Complete	6516	41.9	Microviridae sp.	NA
Microvirus_13	Complete	5845	47.44	NA	Alistipes
Microvirus_14	Complete	5063	43.33	Gokushovirinae sp.	NA
Microvirus_15	Medium-quality	3198	36.59	NA	NA
Microvirus_16	Complete	4891	42.32	Capybara microvirus Cap1_SP_263	NA
Microvirus_17	Complete	6300	38.59	Microviridae sp.	Bacteroides
Microvirus_18	Complete	5873	45.79	Gokushovirus WZ-2015a	Faecalibacterium
Microvirus_19	Complete	5847	43.66	Gokushovirus WZ-2015a	NA
Microvirus_20	Complete	5758	43.4	Gokushovirus WZ-2015a	Faecalibacterium
Microvirus_21	Complete	6720	37.35	Dipodfec virus UOA04_Rod_499	NA
Microvirus_22	Medium-quality	2631	43.18	NA	NA
Microvirus_23	Complete	6037	37.22	Microvirus sp.	NA
Microvirus_24	Complete	6123	35.72	Microvirus sp.	NA
Microvirus_25	High-quality	6775	38.79	Microvirus sp.	Prevotella
Microvirus_26	Complete	4800	45.02	Human gut gokushovirus	NA
Microvirus_27	Low-quality	2125	41.88	Gokushovirus WZ-2015a	NA
Microvirus_28	High-quality	5711	35.95	Microvirus sp.	NA
Microvirus_29	Medium-quality	3568	47.76	Human gut gokushovirus	NA
Microvirus_30	Complete	6963	38.33	Human gut microviridae SH-CHD8	NA
Microvirus_31	Complete	5168	44.54	Microviridae sp.	NA
Microvirus_32	Complete	5176	41	Gokushovirus WZ-2015a	NA
Microvirus_33	Complete	5499	46.79	Dipodfec virus UOA04_Rod_999	Alistipes_A
Microvirus_34	High-quality	5875	45.28	Gokushovirus WZ-2015a	Faecalibacterium
Microvirus_35	Complete	5335	45.74	NA	NA
Microvirus_36	Complete	5536	44.09	Microviridae sp.	Dysosmobacter
Microvirus_37	Medium-quality	3381	38.15	Tortoise microvirus 14	NA
Microvirus_38	Medium-quality	3042	35.77	Gokushovirinae sp.	NA
Microvirus_39	Medium-quality	2986	47.56	Gokushovirus WZ-2015a	NA
Microvirus_40	Complete	5919	45.65	Gokushovirus WZ-2015a	Faecalibacterium
Microvirus_41	Complete	5934	45.8	NA	NA
Microvirus_42	Complete	6619	37.68	Tortoise microvirus 1	NA
Microvirus_43	Complete	5157	41.09	Microviridae sp.	NA
Microvirus_44	Complete	5874	43.65	Gokushovirus WZ-2015a	Faecalibacterium

529 Supplementary table 4: properties of the microviruses found in samples S4 and S18.

530

531 Supplementary table 5: Relative abundance (rel) of each microviral contig in samples S4 and S18
532 before ("raw" column) and after T7pol treatment ("T7pol column").

Sample S4	S4_raw, rel	S4_T7pol, rel	Fold increase
Microvirus_01	1.67E-01	5.53E-01	3.32
Microvirus_02	2.16E-02	5.57E-02	2.58
Microvirus_03	2.11E-02	5.08E-02	2.41
Microvirus_04	1.10E-02	3.24E-02	2.95
Microvirus_05	1.25E-03	2.18E-02	17.47
Microvirus_06	1.31E-02	0	
Microvirus_07	1.21E-03	4.69E-03	3.88
Microvirus_08	1.99E-04	4.59E-03	23.10
Microvirus_09	3.52E-04	3.35E-03	9.52
Microvirus_10	2.82E-04	3.39E-03	12.03
Microvirus_11	3.48E-03	0	
Microvirus_12	2.74E-04	2.47E-03	9.02
Microvirus_13	1.54E-04	1.66E-03	10.81
Microvirus_14	8.25E-05	1.46E-03	17.72
Microvirus_15	1.32E-04	1.10E-03	8.37
Microvirus_16	2.90E-04	9.19E-04	3.17
Microvirus_17	1.65E-04	8.01E-04	4.86
Microvirus_18	7.54E-05	7.94E-04	10.53
Microvirus_19	0	7.65E-04	
Microvirus_20	8.79E-05	5.39E-04	6.13
Microvirus_21	5.84E-05	5.33E-04	9.14
Microvirus_22	1.06E-04	4.28E-04	4.05
Microvirus_23	4.46E-04	0	
Microvirus_24	0	4.44E-04	
Microvirus_25	1.16E-04	3.18E-04	2.75
Microvirus_26	6.33E-05	2.80E-04	4.42
Microvirus_27	0	3.26E-04	
Microvirus_28	6.87E-05	2.32E-04	3.38
Microvirus_29	0	2.98E-04	
Microvirus_30	0	2.65E-04	
Microvirus_31	0	2.50E-04	
Microvirus_32	0	2.50E-04	
Microvirus_33	1.89E-04	0	
Microvirus_34	0	0	
Microvirus_35	0	1.23E-04	
Microvirus_36	1.21E-04	0	
Microvirus_37	1.01E-04	0	
Microvirus_38	0	8.42E-05	
Microvirus_39	0	6.10E-05	
Richness	28	33	
Fold-increase (Average +/-standard deviation)			7.8 +/- 5.71
Sample S18	S18_raw, rel	S18_T7pol, rel	Fold increase
Microvirus_01	0	4.50E-04	
Microvirus_40	9.22E-02	1.70E-01	1.85
Microvirus_41	7.64E-02	5.99E-02	0.78
Microvirus_42	4.91E-02	2.78E-02	0.57
Microvirus_43	2.81E-02	3.11E-02	1.11
Microvirus_44	5.13E-03	1.27E-02	2.48

Microvirus_06	0	3.79E-04	
Microvirus_11	0	1.18E-04	
Richness	5	8	
Fold-increase (Average +/-standard deviation)			1.36 +/- 0.79

533 Supplementary table 6: Relative abundance (rel) of each microviral contig in samples S4 and S18
534 before ("raw" column) and after T7pol treatment ("T7pol column").

Contig name	S4_raw, rel	S4_T7pol, rel	Contig name	S18_raw, rel	S18_T7pol, rel
Caudoviricetes_01	9.72E-02	6.13E-02	Caudoviricetes_148	2.88E-01	1.74E-01
Caudoviricetes_02	6.70E-02	3.31E-02	Caudoviricetes_03	1.94E-01	2.49E-01
Caudoviricetes_03	4.35E-02	1.79E-02	Caudoviricetes_149	2.97E-02	1.45E-02
Caudoviricetes_04	2.16E-02	1.62E-02	Caudoviricetes_150	1.35E-02	1.12E-02
Caudoviricetes_05	2.04E-02	1.22E-02	Caudoviricetes_151	7.21E-03	7.82E-03
Caudoviricetes_06	1.80E-02	7.85E-03	Caudoviricetes_152	4.35E-03	4.49E-03
Caudoviricetes_07	2.06E-02	4.53E-03	Caudoviricetes_153	4.31E-03	3.37E-03
Caudoviricetes_08	2.14E-02	0	Caudoviricetes_154	2.19E-03	4.04E-03
Caudoviricetes_09	1.56E-02	1.18E-04	Caudoviricetes_155	2.68E-03	3.10E-03
Caudoviricetes_10	1.31E-02	2.47E-03	Caudoviricetes_156	2.26E-03	2.49E-03
Caudoviricetes_11	1.51E-02	0.00E+00	Caudoviricetes_157	2.21E-03	2.31E-03
Caudoviricetes_12	1.29E-02	2.82E-04	Caudoviricetes_158	2.28E-03	1.23E-03
Caudoviricetes_13	1.02E-02	2.50E-03	Caudoviricetes_159	1.53E-03	1.40E-03
Caudoviricetes_14	9.87E-03	2.39E-03	Caudoviricetes_160	1.03E-03	1.69E-03
Caudoviricetes_15	9.52E-03	2.65E-03	Caudoviricetes_161	9.80E-04	1.34E-03
Caudoviricetes_16	9.60E-03	2.41E-03	Caudoviricetes_162	6.30E-04	9.22E-04
Caudoviricetes_17	9.46E-03	2.28E-03	Caudoviricetes_163	7.34E-04	4.88E-04
Caudoviricetes_18	9.08E-03	2.29E-03	Caudoviricetes_164	3.09E-04	7.55E-04
Caudoviricetes_19	9.25E-03	2.02E-03	Caudoviricetes_165	5.87E-04	4.68E-04
Caudoviricetes_20	8.88E-03	2.15E-03	Caudoviricetes_08	0	9.05E-04
Caudoviricetes_21	7.00E-03	3.88E-03	Caudoviricetes_166	4.71E-04	4.10E-04
Caudoviricetes_22	7.28E-03	3.29E-03	Caudoviricetes_167	2.89E-04	5.81E-04
Caudoviricetes_23	8.56E-03	1.93E-03	Caudoviricetes_168	4.23E-04	4.18E-04
Caudoviricetes_24	8.63E-03	1.62E-03	Caudoviricetes_169	3.33E-04	4.35E-04
Caudoviricetes_25	6.48E-03	1.41E-03	Caudoviricetes_170	3.64E-04	3.36E-04
Caudoviricetes_26	6.87E-03	2.82E-04	Caudoviricetes_171	3.14E-04	3.58E-04
Caudoviricetes_27	6.75E-03	3.38E-04	Caudoviricetes_172	2.30E-04	4.35E-04
Caudoviricetes_28	6.38E-03	0	Caudoviricetes_173	2.63E-04	3.83E-04
Caudoviricetes_29	4.80E-03	1.24E-03	Caudoviricetes_174	3.18E-04	3.14E-04
Caudoviricetes_30	4.69E-03	1.03E-03	Caudoviricetes_175	2.61E-04	3.48E-04
Caudoviricetes_31	5.63E-03	0	Caudoviricetes_176	2.92E-04	3.15E-04
Caudoviricetes_32	5.62E-03	0	Caudoviricetes_177	2.31E-04	3.72E-04
Caudoviricetes_33	3.85E-03	7.24E-04	Caudoviricetes_178	2.54E-04	3.01E-04
Caudoviricetes_34	2.58E-03	1.50E-03	Caudoviricetes_179	2.60E-04	2.81E-04
Caudoviricetes_35	3.46E-03	0	Caudoviricetes_180	1.65E-04	3.65E-04
Caudoviricetes_36	1.74E-03	1.38E-03	Caudoviricetes_181	1.97E-04	3.33E-04
Caudoviricetes_37	2.23E-03	7.15E-04	Caudoviricetes_182	3.21E-04	2.02E-04
Caudoviricetes_38	2.66E-03	0	Caudoviricetes_183	1.23E-04	3.89E-04
Caudoviricetes_39	2.63E-03	0	Caudoviricetes_184	3.50E-04	1.60E-04
Caudoviricetes_40	2.05E-03	4.67E-04	Caudoviricetes_185	1.68E-04	3.42E-04

Caudoviricetes_41	2.36E-03	0	Caudoviricetes_186	1.93E-04	3.08E-04
Caudoviricetes_42	1.52E-03	8.06E-04	Caudoviricetes_187	2.97E-04	2.00E-04
Caudoviricetes_43	2.23E-03	0	Caudoviricetes_188	1.76E-04	3.18E-04
Caudoviricetes_44	2.17E-03	0	Caudoviricetes_09	0	4.88E-04
Caudoviricetes_45	2.15E-03	0	Caudoviricetes_189	3.44E-04	1.43E-04
Caudoviricetes_46	9.47E-04	7.54E-04	Caudoviricetes_11	0	4.82E-04
Caudoviricetes_47	1.69E-03	0	Caudoviricetes_190	3.37E-04	1.38E-04
Caudoviricetes_48	8.93E-04	7.49E-04	Caudoviricetes_191	2.23E-04	2.43E-04
Caudoviricetes_49	1.14E-03	3.89E-04	Caudoviricetes_192	3.00E-04	1.52E-04
Caudoviricetes_50	1.52E-03	0	Caudoviricetes_193	2.20E-04	2.30E-04
Caudoviricetes_51	9.71E-04	5.34E-04	Caudoviricetes_194	1.69E-04	2.70E-04
Caudoviricetes_52	1.34E-03	0	Caudoviricetes_195	2.83E-04	1.54E-04
Caudoviricetes_53	8.29E-04	4.72E-04	Caudoviricetes_196	2.19E-04	1.99E-04
Caudoviricetes_54	6.25E-04	6.66E-04	Caudoviricetes_197	1.80E-04	2.32E-04
Caudoviricetes_55	1.20E-03	0	Caudoviricetes_198	1.62E-04	2.41E-04
Caudoviricetes_56	1.01E-03	1.77E-04	Caudoviricetes_199	1.84E-04	2.13E-04
Caudoviricetes_57	1.03E-03	0	Caudoviricetes_200	2.34E-04	1.60E-04
Caudoviricetes_58	8.01E-04	2.05E-04	Caudoviricetes_201	1.54E-04	2.37E-04
Caudoviricetes_59	9.98E-04	0	Caudoviricetes_202	1.44E-04	2.39E-04
Caudoviricetes_60	8.26E-04	1.56E-04	Caudoviricetes_203	1.81E-04	1.98E-04
Caudoviricetes_61	9.52E-04	0	Caudoviricetes_204	1.96E-04	1.80E-04
Caudoviricetes_62	9.28E-04	0	Caudoviricetes_205	2.02E-04	1.62E-04
Caudoviricetes_63	6.60E-04	2.44E-04	Caudoviricetes_206	1.96E-04	1.62E-04
Caudoviricetes_64	8.32E-04	0	Caudoviricetes_12	0	3.53E-04
Caudoviricetes_65	5.15E-04	2.72E-04	Caudoviricetes_207	2.13E-04	1.40E-04
Caudoviricetes_66	4.85E-04	3.00E-04	Caudoviricetes_208	1.83E-04	1.64E-04
Caudoviricetes_67	4.75E-04	2.96E-04	Caudoviricetes_209	1.84E-04	1.61E-04
Caudoviricetes_68	7.45E-04	0	Caudoviricetes_210	1.72E-04	1.71E-04
Caudoviricetes_69	7.07E-04	0	Caudoviricetes_211	3.38E-04	0
Caudoviricetes_70	6.94E-04	0	Caudoviricetes_212	1.08E-04	2.27E-04
Caudoviricetes_71	3.86E-04	2.95E-04	Caudoviricetes_213	1.65E-04	1.65E-04
Caudoviricetes_72	6.28E-04	0	Caudoviricetes_214	1.51E-04	1.68E-04
Caudoviricetes_73	4.32E-04	1.68E-04	Caudoviricetes_215	1.84E-04	1.32E-04
Caudoviricetes_74	3.60E-04	2.32E-04	Caudoviricetes_216	1.49E-04	1.63E-04
Caudoviricetes_75	5.89E-04	0	Caudoviricetes_217	1.39E-04	1.72E-04
Caudoviricetes_76	4.07E-04	1.58E-04	Caudoviricetes_218	1.45E-04	1.66E-04
Caudoviricetes_77	5.33E-04	0	Caudoviricetes_219	1.27E-04	1.83E-04
Caudoviricetes_78	5.30E-04	0	Caudoviricetes_220	1.43E-04	1.56E-04
Caudoviricetes_79	5.29E-04	0	Caudoviricetes_221	2.90E-04	0
Caudoviricetes_80	2.98E-04	2.21E-04	Caudoviricetes_222	1.31E-04	1.57E-04
Caudoviricetes_81	3.32E-04	1.34E-04	Caudoviricetes_223	1.21E-04	1.66E-04
Caudoviricetes_82	2.68E-04	1.89E-04	Caudoviricetes_224	1.19E-04	1.68E-04
Caudoviricetes_83	2.48E-04	2.03E-04	Caudoviricetes_225	1.58E-04	1.21E-04
Caudoviricetes_84	3.58E-04	8.26E-05	Caudoviricetes_226	1.26E-04	1.52E-04
Caudoviricetes_85	4.14E-04	0	Caudoviricetes_227	1.50E-04	1.27E-04
Caudoviricetes_86	4.00E-04	0	Caudoviricetes_228	1.35E-04	1.35E-04
Caudoviricetes_87	3.76E-04	0	Caudoviricetes_28	0	2.67E-04

Caudoviricetes_88	3.75E-04	0
Caudoviricetes_89	2.14E-04	1.61E-04
Caudoviricetes_90	3.60E-04	0
Caudoviricetes_91	1.40E-04	2.09E-04
Caudoviricetes_92	1.96E-04	1.31E-04
Caudoviricetes_93	1.93E-04	1.33E-04
Caudoviricetes_94	2.87E-04	0
Caudoviricetes_95	2.30E-04	4.04E-05
Caudoviricetes_96	2.66E-04	0
Caudoviricetes_97	2.52E-04	0
Caudoviricetes_98	2.47E-04	0
Caudoviricetes_99	1.19E-04	1.26E-04
Caudoviricetes_100	1.59E-04	7.98E-05
Caudoviricetes_101	2.35E-04	0
Caudoviricetes_102	2.30E-04	0
Caudoviricetes_103	1.73E-04	4.99E-05
Caudoviricetes_104	2.19E-04	0
Caudoviricetes_105	2.17E-04	0
Caudoviricetes_106	2.14E-04	0
Caudoviricetes_107	1.51E-04	5.07E-05
Caudoviricetes_108	1.31E-04	6.64E-05
Caudoviricetes_109	1.33E-04	5.48E-05
Caudoviricetes_110	1.04E-04	7.87E-05
Caudoviricetes_111	1.78E-04	0
Caudoviricetes_112	1.68E-04	0
Caudoviricetes_113	1.66E-04	0
Caudoviricetes_114	1.53E-04	0
Caudoviricetes_115	1.43E-04	0
Caudoviricetes_116	8.00E-05	6.25E-05
Caudoviricetes_117	1.42E-04	0
Caudoviricetes_118	1.40E-04	0
Caudoviricetes_119	9.09E-05	4.29E-05
Caudoviricetes_120	6.67E-05	5.28E-05
Caudoviricetes_121	1.10E-04	0
Caudoviricetes_122	1.06E-04	0
Caudoviricetes_123	4.95E-05	5.23E-05
Caudoviricetes_124	9.78E-05	0
Caudoviricetes_125	9.45E-05	0
Caudoviricetes_126	9.40E-05	0
Caudoviricetes_127	9.38E-05	0
Caudoviricetes_128	8.30E-05	0
Caudoviricetes_129	8.14E-05	0
Caudoviricetes_130	6.80E-05	0
Caudoviricetes_131	6.64E-05	0
Caudoviricetes_132	6.63E-05	0
Caudoviricetes_133	6.36E-05	0
Caudoviricetes_134	6.31E-05	0

Caudoviricetes_229	1.37E-04	1.21E-04
Caudoviricetes_230	9.24E-05	1.47E-04
Caudoviricetes_231	1.45E-04	8.69E-05
Caudoviricetes_31	0	2.08E-04
Caudoviricetes_232	1.22E-04	8.48E-05
Caudoviricetes_233	1.04E-04	1.03E-04
Caudoviricetes_234	2.00E-04	0
Caudoviricetes_235	8.86E-05	1.09E-04
Caudoviricetes_32	0	1.92E-04
Caudoviricetes_236	1.87E-04	0
Caudoviricetes_237	1.71E-04	0
Caudoviricetes_238	1.69E-04	0
Caudoviricetes_39	0	1.58E-04
Caudoviricetes_239	1.51E-04	0
Caudoviricetes_27	0	1.40E-04
Caudoviricetes_35	0	1.38E-04
Caudoviricetes_240	0	1.36E-04
Caudoviricetes_26	0	1.35E-04
Caudoviricetes_241	1.23E-04	0
Caudoviricetes_242	0	1.22E-04
Caudoviricetes_243	1.13E-04	0
Caudoviricetes_244	1.10E-04	0
Caudoviricetes_245	0	1.10E-04
Caudoviricetes_246	0	1.06E-04
Caudoviricetes_247	0	9.79E-05
Caudoviricetes_248	0	9.20E-05
Caudoviricetes_43	0	8.68E-05
Caudoviricetes_249	0	7.20E-05
Caudoviricetes_250	1.93E-05	4.11E-05
Caudoviricetes_59	0	3.21E-05
Caudoviricetes_251	2.90E-05	0

Caudoviricetes_135	5.97E-05	0
Caudoviricetes_136	0	5.06E-05
Caudoviricetes_137	0	4.60E-05
Caudoviricetes_138	0	4.25E-05
Caudoviricetes_139	0	4.25E-05
Caudoviricetes_140	0	3.80E-05
Caudoviricetes_141	0	3.58E-05
Caudoviricetes_142	0	3.54E-05
Caudoviricetes_143	0	3.40E-05
Caudoviricetes_144	0	3.28E-05
Caudoviricetes_145	0	3.23E-05
Caudoviricetes_146	1.81E-05	0

537

538 Supplementary figure 1: pipeline of virome reads analysis

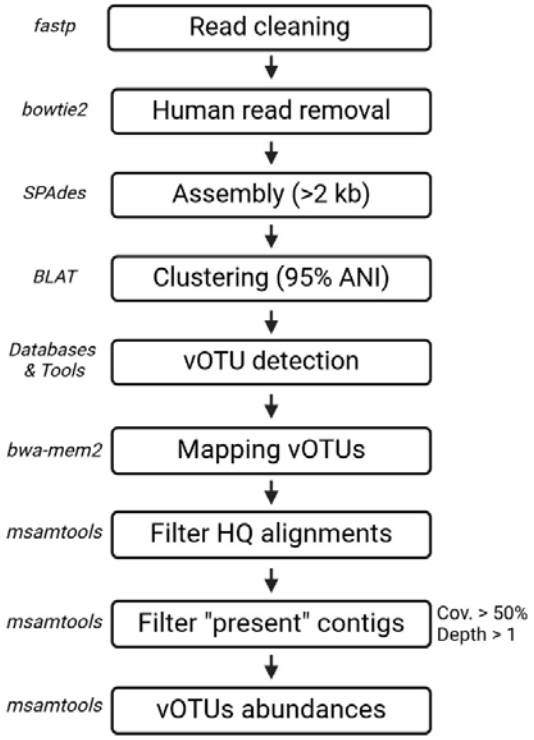

539

540

Supplementary figure 2: raw gel of figure 1

Supplementary figure 3: raw gel of figure 2.

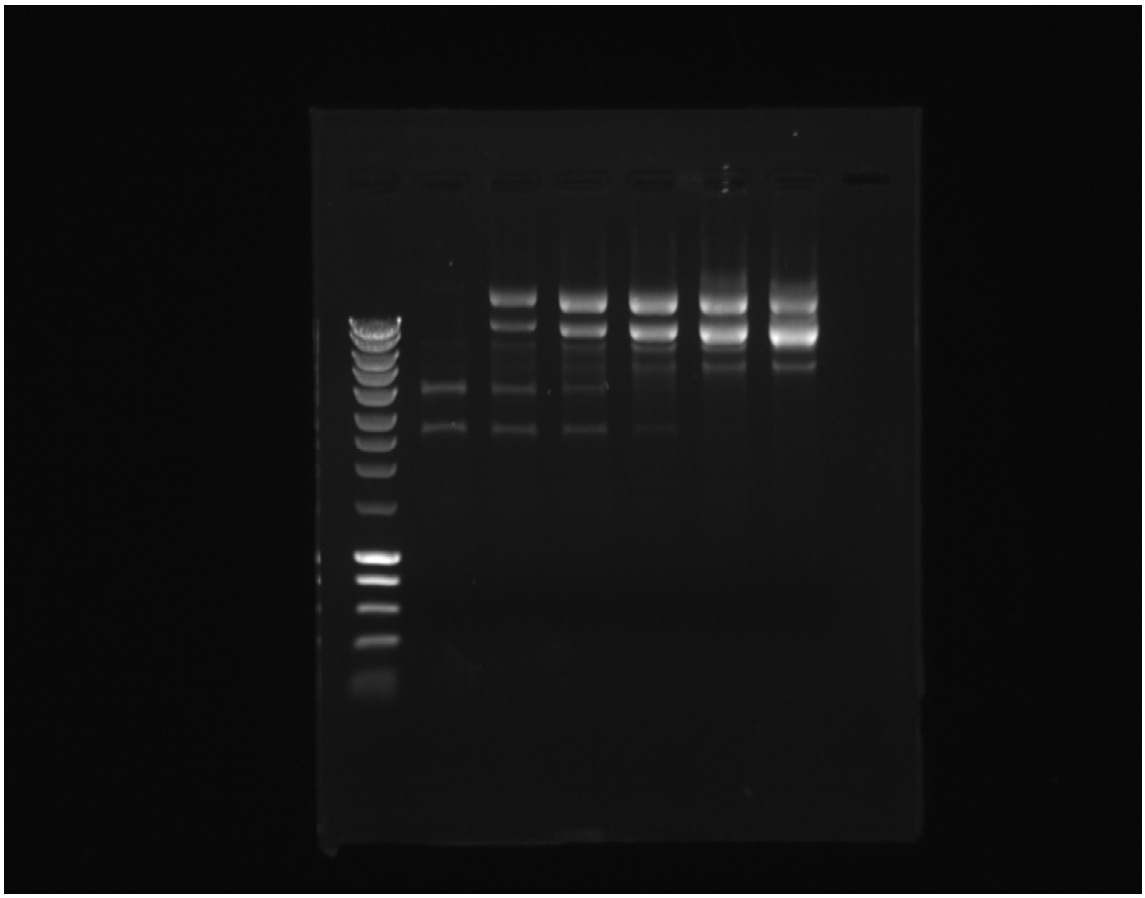

Supplementary figure 4: Relative abundance of each *Caudoviricetes* detected in samples S4 (top) and S18 (bottom). Each dot represents one contig, with its abundance relative to all phages of the sample when sequenced without prior treatment for ssDNA (X axis) or after T7pol treatment (Y axis). The dotted line shows the bisector. Contigs undetected with one of the treatments were assigned an artificial value of 10^{-5}.

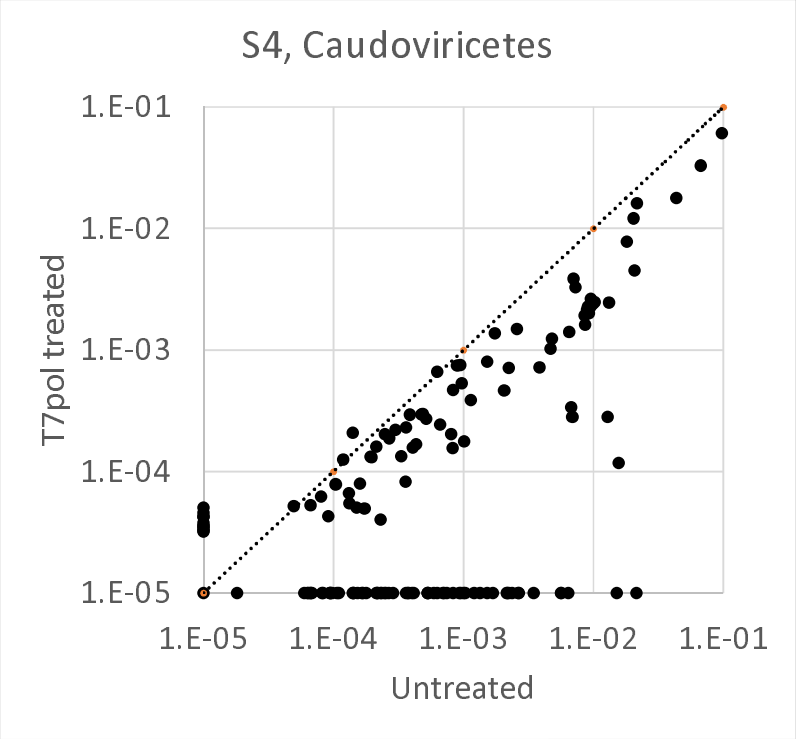

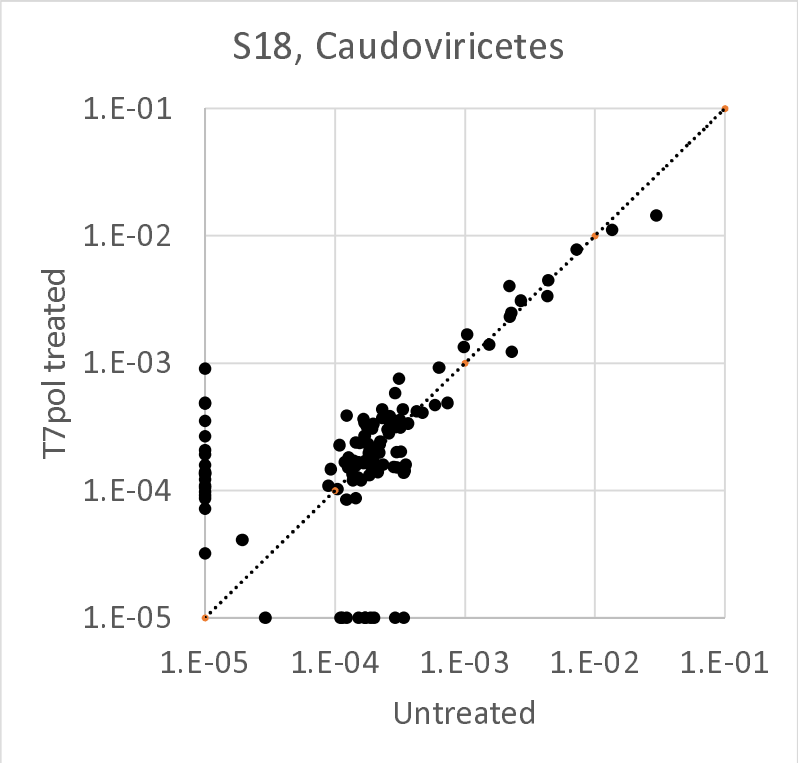

579

580 Supplementary figure 5: VipTree classification of the microviruses detected in samples S4 and S18.

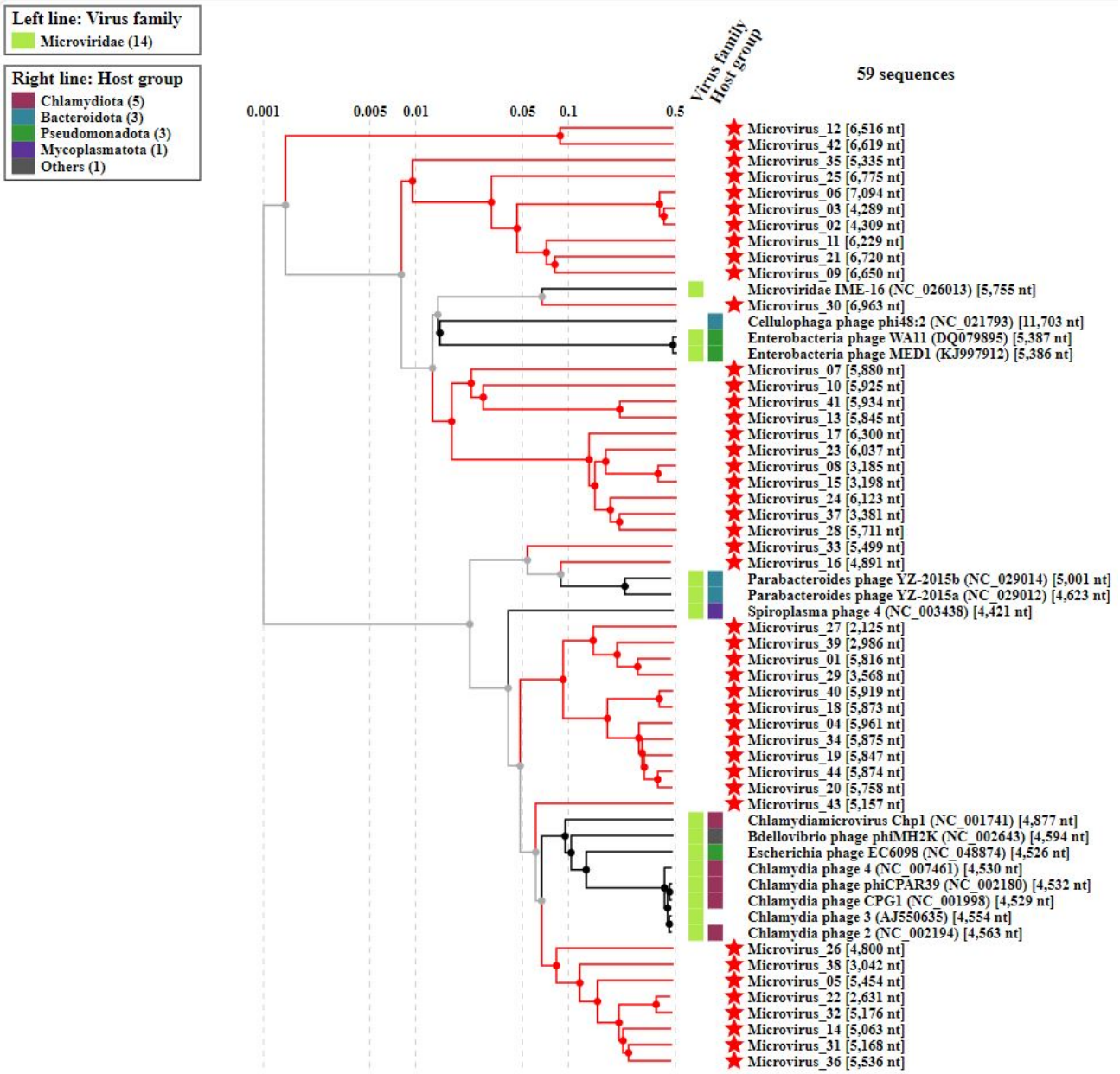

581

	Rep. 1				Rep. 2				
	ds	ss	ds**B**	ss**B**	ds	ss	ds**B**	ss**B**	
Length (nt, max. intensity)	566	316	522	418	330	235	325	325	M (nt)

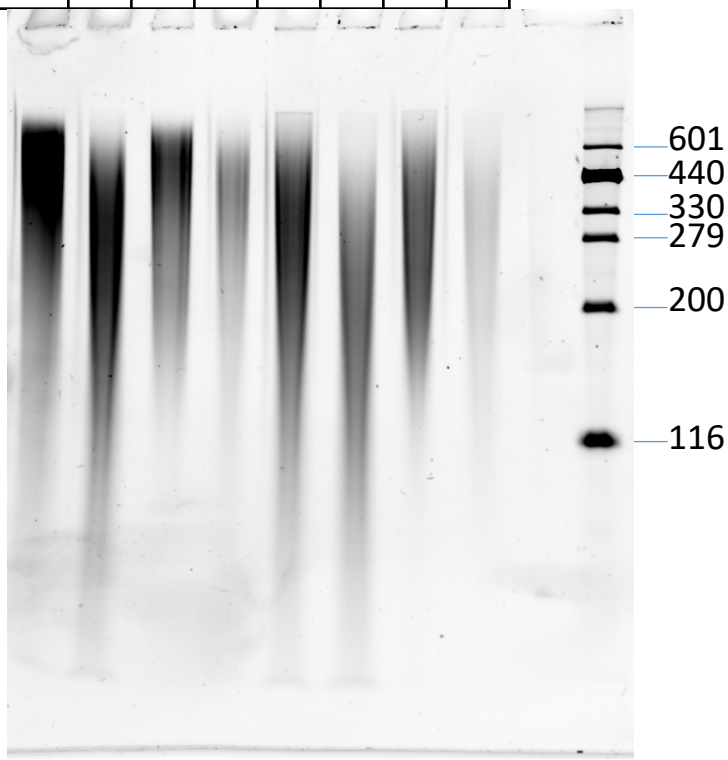

Figure 1

A

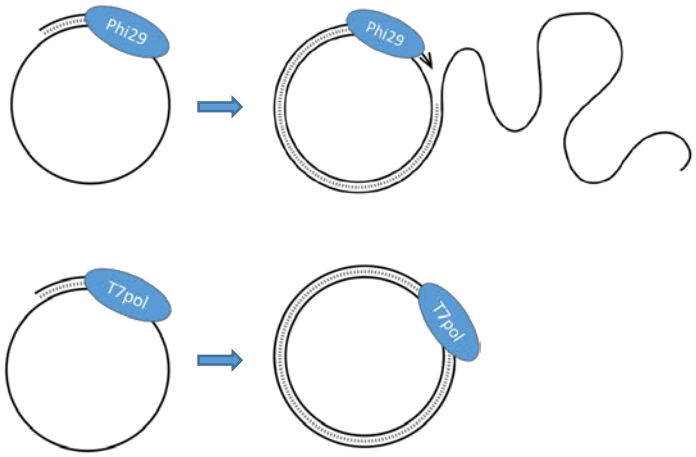
Phi29
Phi29
T7pol
T7pol

B

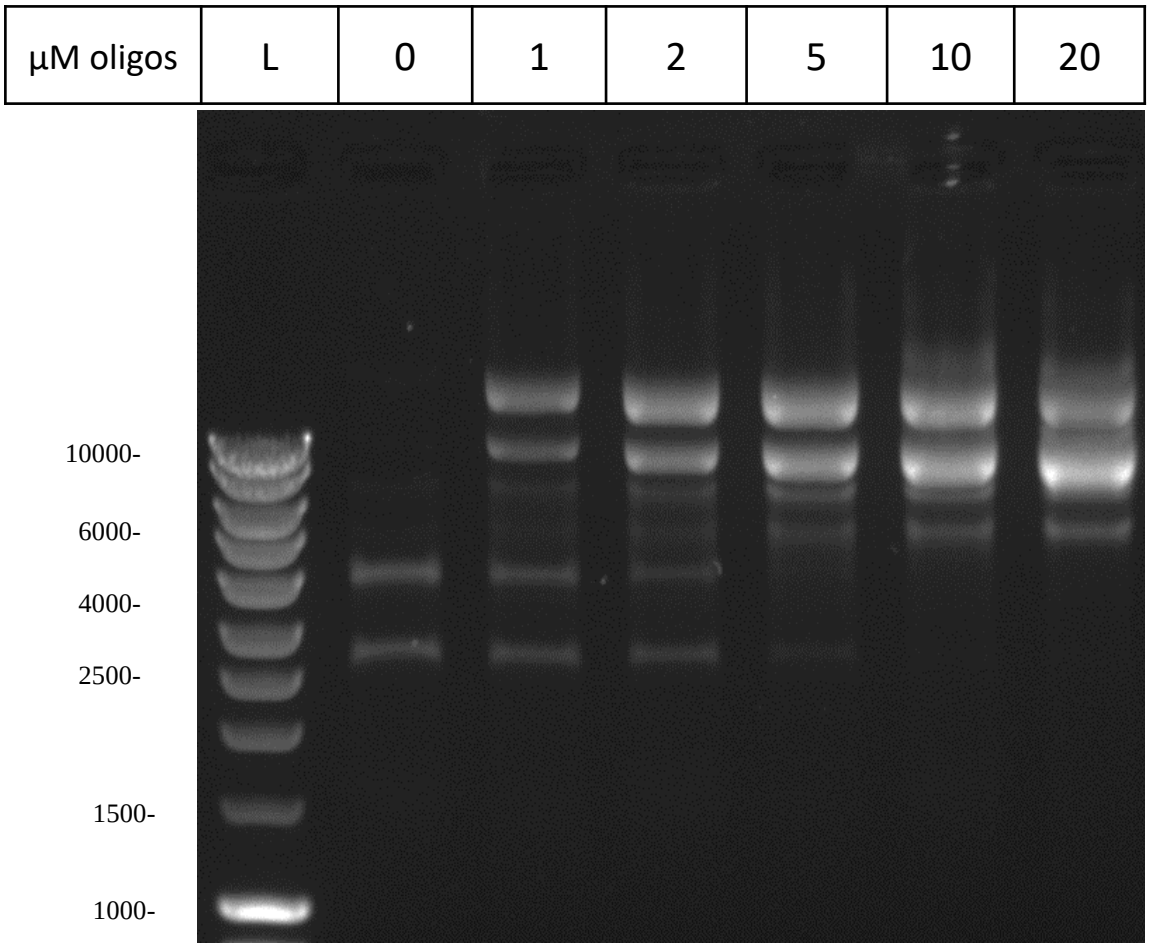
µM oligos
L
0
1
2
5
10
20
10000-
6000-
4000-
2500-
1500-
1000-

Figure 2

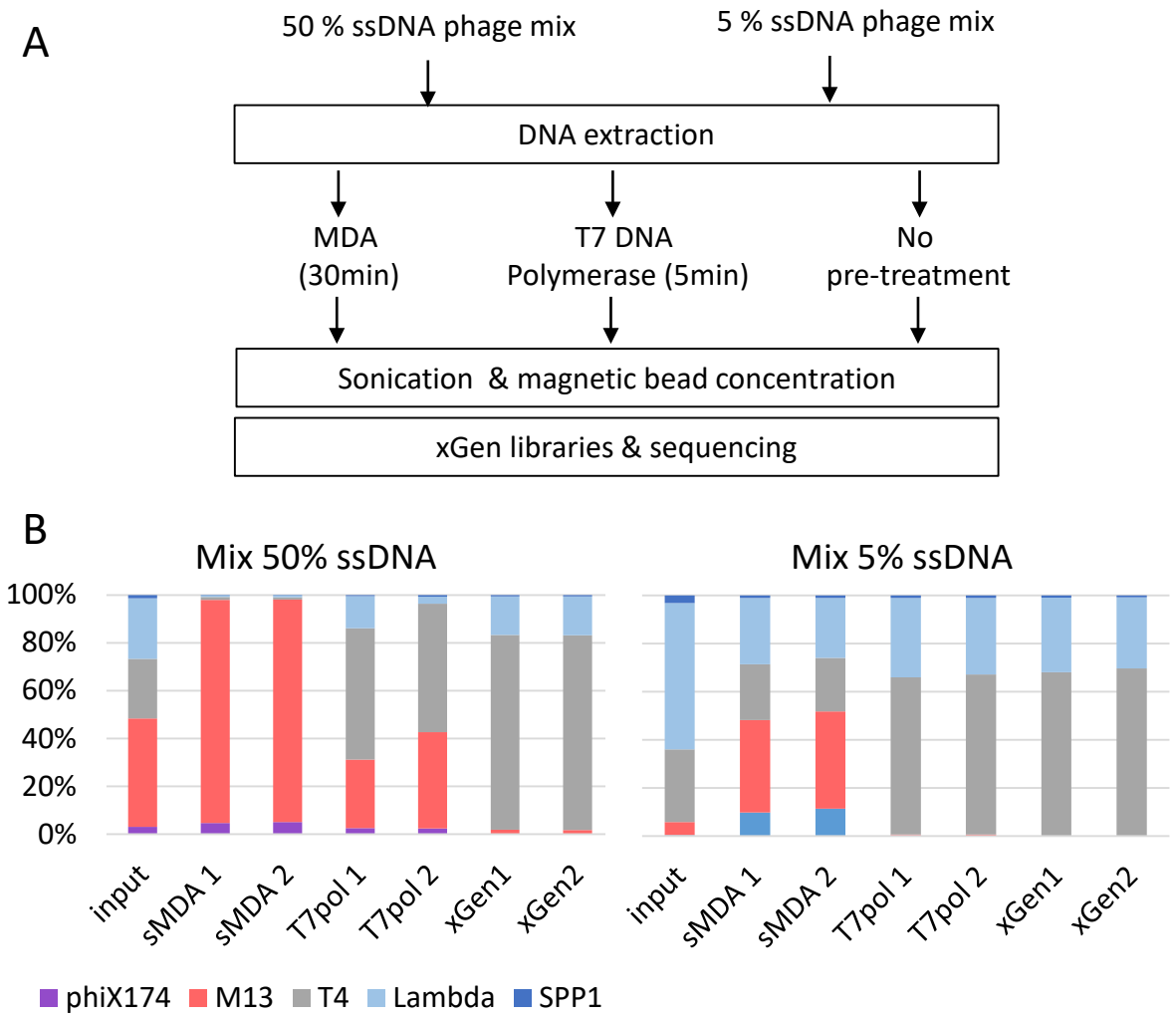
A
50 % ssDNA phage mix
5 % ssDNA phage mix
DNA extraction
MDA
(30min)
T7 DNA
Polymerase (5min)
No
pre-treatment
Sonication & magnetic bead concentration
xGen libraries & sequencing
B
Mix 50% ssDNA
Mix 5% ssDNA
100%
80%
60%
40%
20%
0%
input
sMDA 1
sMDA 2
T7pol 1
T7pol 2
xGen1
xGen2
phiX174
M13
T4
Lambda
SPP1

Figure 3

A

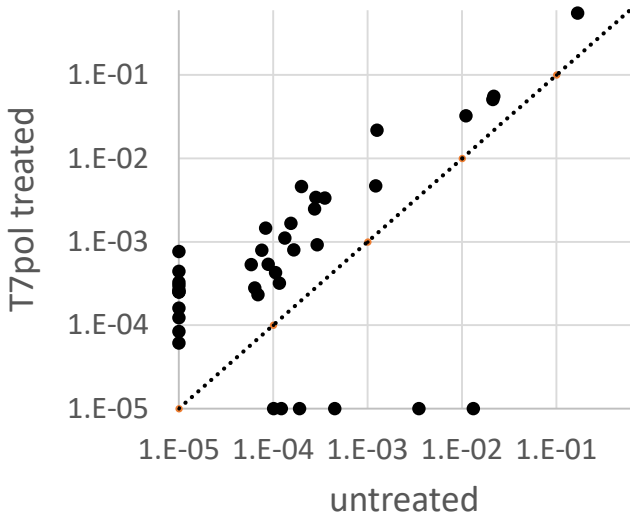
T7pol treated
1.E-01
1.E-02
1.E-03
1.E-04
1.E-05
1.E-05 1.E-04 1.E-03 1.E-02 1.E-01
untreated

B

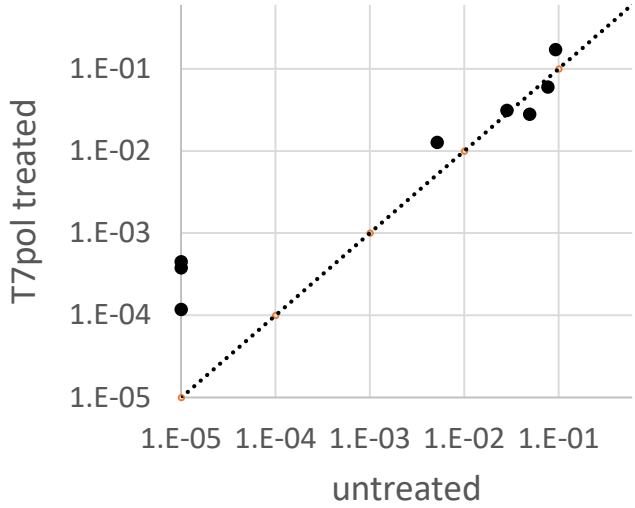
T7pol treated
1.E-01
1.E-02
1.E-03
1.E-04
1.E-05
1.E-05 1.E-04 1.E-03 1.E-02 1.E-01
untreated

Figure 4